Chapter 7A. Summary of the Haji-Gak Iron Area of Interest

Contribution by Karine Renaud, David M. Sutphin, Stephen G. Peters, and Lawrence J. Drew

Abstract

The Haji-Gak iron area of interest in Bamyan, Parwan, and Wardak Provinces contains the Haji-Gak iron deposit and several other prospects and deposits. Three subareas have been delineated within the main area of interest. The Haji-Gak iron deposit (prospect subarea) in Bamyan Province is the best known and largest iron oxide deposit in Afghanistan. The Haji-Gak ore deposit is more than 12 kilometers (km) long and 3 kilometers (km) wide and contains 16 separate zones, some of which are as much as 5 km in length, 380 meters (m) wide and extend 550 m downdip. Seven of these zones have been studied in detail. Iron ore is primary and oxide. The primary ore [80 volume percent (vol. %) of the deposit] is present below 130 m, comprises mostly magnetite and pyrite as well as smaller amounts of other sulfide minerals, including chalcopyrite, and averages 61.3 weight percent (wt. %) iron. The remaining 20 vol. % of the iron ore is oxidized and consists of three hematitic ore types at slightly higher grades (more than 62.0 wt. %). The mineralization is structurally controlled. A previous Russian resource estimate for the entire deposit is 1,700 million metric tons (Mt), although the mining reserve estimate for the near surface oxide ore in the most explored area is 85 Mt.

The Chuy, Khaish, Khakriz, Kharzar, and Zerak sedimentary-rock-hosted iron deposits are adjacent and to the east of the main Haji-Gak iron deposit in the Northeastern Haji-Gak subarea and have also been explored. The Haji-Gak iron area of interest also contains barite deposits and mineralization near the Haji-Gak prospect subarea and in the Northeastern and Farenjal subareas. The Haji-Gak barite deposit in the Haji-Gak prospect subarea fills veins over an area of 10 square kilometers (km^2). The speculative resources of the largest vein are 36,200 metric tons with an average barium oxide content of 56 wt. % barium oxide. Additionally, the Haji-Gak prospect subarea contains the Haji-Gak limestone deposit with speculative resources over an area of 45 km^2 to a depth of 60 m and reported resource of 3.5 Mt. The Haji-Gak sandstone, also in the Haji-Gak prospect subarea, grades from 93.66 to 97.31 wt. % silicon oxide and contains speculative resource of 650,000 metric tons. Speculative resources are undiscovered resources that occur in unknown and undiscovered types of deposits in favorable geologic settings or in unknown types of deposits that have to be recognized. The quality of the silicon oxide raw material is suitable for manufacturing class-II dinas.

In the northeastern part of the Haji-Gak iron area of interest, Paleozoic strata contain the Farenjal barite and lead-zinc ore district. The subordinate mineralization consists of asbestos, copper, iron, manganese, and talc.

Extensive exploration has been done in the Haji-Gak prospect subarea for iron deposits. Afghan, French, German, and Russian feasibility studies on the main iron deposit were completed. The remainder of the Haji-Gak iron area of interest has not been explored to this level. A U.S. Geological Survey team visited the lower parts of the ore deposit area briefly in 2006 and 2009.

7A.1 Introduction

This chapter is a summary and interpretation of Kusov and others (1965b), correlating the report with the results of joint geologic and compilation activities conducted during 2009 to 2011 by the U.S. Geological Survey (USGS), the U.S. Department of Defense Task Force for Business and Stability Operations (TFBSO), and the Afghanistan Geological Survey (AGS) (fig. 7A–1; table 7A–1) in the Haji-Gak iron area of interest (AOI) and subareas. Accompanying complementary chapters 7B, 7C, and 7D additionally address hyperspectral data, geohydrologic, and ore reserve assessments respectively of

the Haji-Gak iron AOI. Supporting AOI data and information for this chapter are available from the Ministry of Mines in Kabul.

We have attempted to translate the original Russian terminology and rock classification into modern English geologic usage as literally as possible without changing any implied genetic or process oriented implications in the original descriptions, using the age presented in the original report. A more recent study of the Haji-Gak area (Kusov, 1965a) substantially modified the ages for the Haji-Gak Formation from Proterozoic to Devonian and provided new interpretations of the geologic settings in which various units were deposited.

The Haji-Gak iron AOI is in east-central Afghanistan and consists of a main area and three subareas. The main area is 2,079 square kilometers (km^2) the Farenjal subarea is 557 km^2, the Northeast (NE) Haji-Gak subarea is 381 km^2, and the Haji-Gak prospect subarea is 180 km^2 (fig. 7A–2). The Haji-Gak iron AOI is located in parts of the Bamyan, Parwan, and Wardak Provinces and parts of the Bamyan, Beshud, Ghorband, Hisa-i-Awal, Markazi, Shekh Ali, Shibar, and Surkh-i-Parso Districts. Deposit types that are expected or known in the Haji-Gak iron AOI are Algoma iron, bedded barite, sandstone, and limestone.

7A.2 Previous Work

The Haji-Gak iron deposit has been explored since 1911, and geologic and engineering work has been summarized in many Soviet reports; however, modern reconnaissance and prospecting work did not start until 1965. The first recorded geologic exploration was by G. Hyden, Director of the Geological Survey of India, who explored the Haji-Gak iron deposit for the first time in 1911. During this expedition, a stratigraphic sequence for the area was constructed, and three formations were identified, along with their ages; the formations were Kalu (Awband Formation) of Early Devonian age, Haji-Gak of Devonian age, and Helmand of Carbonaceous age.

The Haji-Gak iron deposit was further investigated by K. Brueckl (1935, 1936), Popol and Tromb (1954), Bybochkin and Kurotchenko (1960), Momji and Chaikin (1960), de Lapparent (1961), and Mirzad (1961).

In Brueckl (1935, 1936) the hydrothermal siderite veins in the deposit and the hornblende granitic intrusion that was cut by these siderite veins were described and categorized. Brueckl (1935, 1936) proposed that formation of magmatic hydrothermal siderite veins, and by inference the iron ores, were genetically and spatially related to the granite. The hypotheses on iron ore genesis were bolstered by Bybochkin and Kurotchenko (1960) and Momji and Chaikin (1960).

Table 7A–1. Reserves and resources of the Haji-Gak iron deposit.
[Tabulation of data from Soviet exploration in the 1960s. NA, not available]

Soviet category	Equivalent classification	Ore type	Reserve, million metric tons of ore	Iron, weight percent	Sulfur, weight percent
A	Measured or proven	Oxidized ore	9.1	62.52	0.14
B	Measured or proven	Oxidized ore	19.2	62.69	0.09
C_1	Indicated or probable	Oxidized ore	65.1	62.15	0.13
C_1	Indicated or probable	Primary ore	16.2	61.3	4.56
C_1	Indicated or probable	Fragmental ore	1.2	60.62	0.08
C_2	Inferred or possible	All ore types	3,143	NA	NA
C_2	Inferred or possible	Fragmental ore	2.9	NA	NA
P_2	Hypothetical resources	All ore types	1,333.3	NA	NA
P_2	Hypothetical resources	Fragmental ore	8.6	NA	NA
	Total		1,769.9		

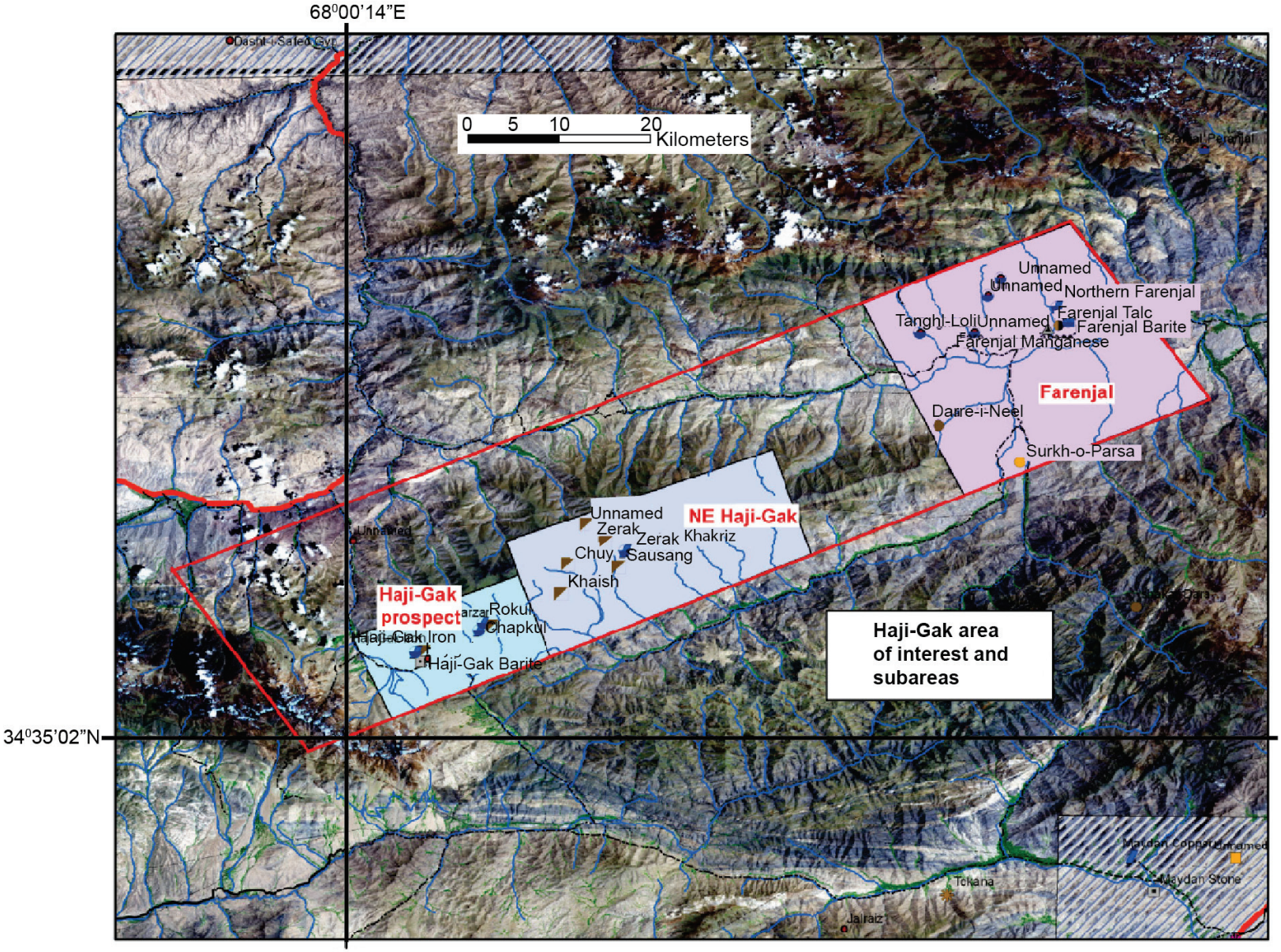

Figure 7A–1. LANDSAT image of the Haji-Gak iron area of interest (outlined in red), showing subareas (color-shaded areas) and major prospects (brown and blue triangles) and mineral occurrences (red and yellow circles). Data are from Peters and others (2007, p. 118–122).

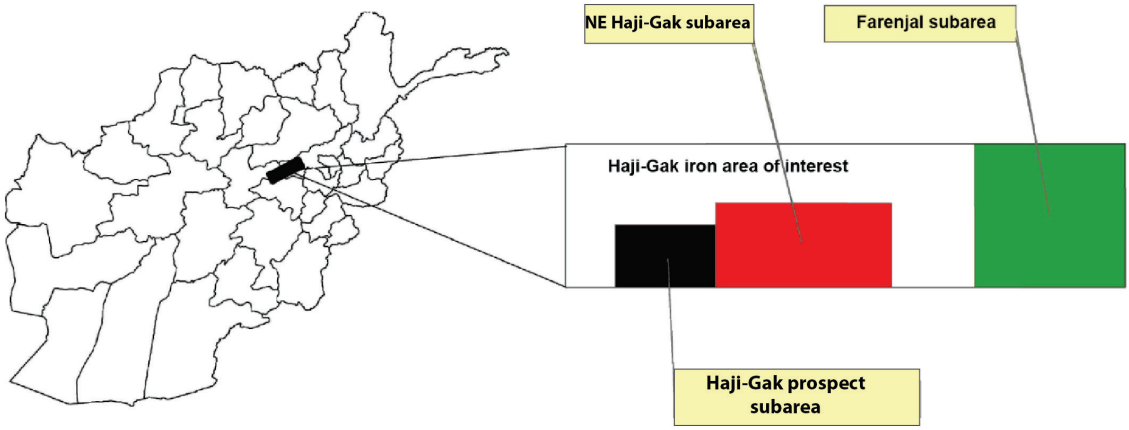

Figure 7A–2. Map showing the location of the Haji-Gak area of interest and subareas.

Popol and Tromb (1954) identified schist and three sedimentary sequences (from top to bottom), as follows: schist and limestone, red layers, and coarse-grained conglomerate. Devonian fauna was found in limestone. These sequences overlay the Kalu Formation that is in turn overlain by the Helmand Formation.

In de Lapparent, (1961) the Haji-Gak iron deposit was identified as an exhalative deposit, which suggested the deposit had undergone two types of metamorphism—greenschist facies and sericite dynamic-metamorphism.

The most extensive information about the deposit and its resources was provided by Momji and Chaikin (1961), Bybochkin and Kurotchenko (1961), and Mirzad (1961).

Most of the detailed prospecting has been done on the western part of Haji-Gak iron mineralized zone. This work was carried out by Russian and Afghan geologists and has been documented in many reports listed in the Selected References section of this chapter. This exploration is well documented by Kusov and others (1965a,b) and includes prospect and geological maps at different scales (fig. 7A–3). The work included the drilling of 4 holes, opening of 15 adits and 29 trenches, and hand specimen and microscopic description of ores and minerals, calculation of ore reserves, and the study of hydrogeology of the region.

Exploration and geologic work terminated in 1989 with the withdrawal of the Soviet army and the civil war that interrupted further activity by the Afghanistan Geological Survey (AGS). Although the AGS was able to preserve many of the Soviet reports, some of the reports were destroyed. The condition of the reports and maps ranges from poor to excellent.,

7A.3 Metallogeny

Iron deposits hosted in sedimentary rocks in Afghanistan mainly are present within Proterozoic sedimentary and volcanic-sedimentary rock packages (Peters and others, 2007, p. 118–122). Most iron deposits, including the large Haji-Gak iron ore deposit and its associated deposits, are present along a tectonized zone in the Har-i-Rod Fault zone in central Afghanistan. Additionally, an oolitic ironstone mineral occurrence also is known in the Late Paleozoic to Cenozoic sedimentary rocks (Nishiwak, 1970). Hematite vein deposits also are present in Proterozoic, Permian, and Oligocene rocks. Other major iron deposits in Afghanistan are in iron skarn bodies mainly around Oligocene intrusive bodies in the Kandahar and Badakshan Provinces. Some geologists believe that the Proterozoic-hosted deposits are products of contact metamorphism around the Oligocene intrusive bodies (Peters and others, 2007, p. 118–122).

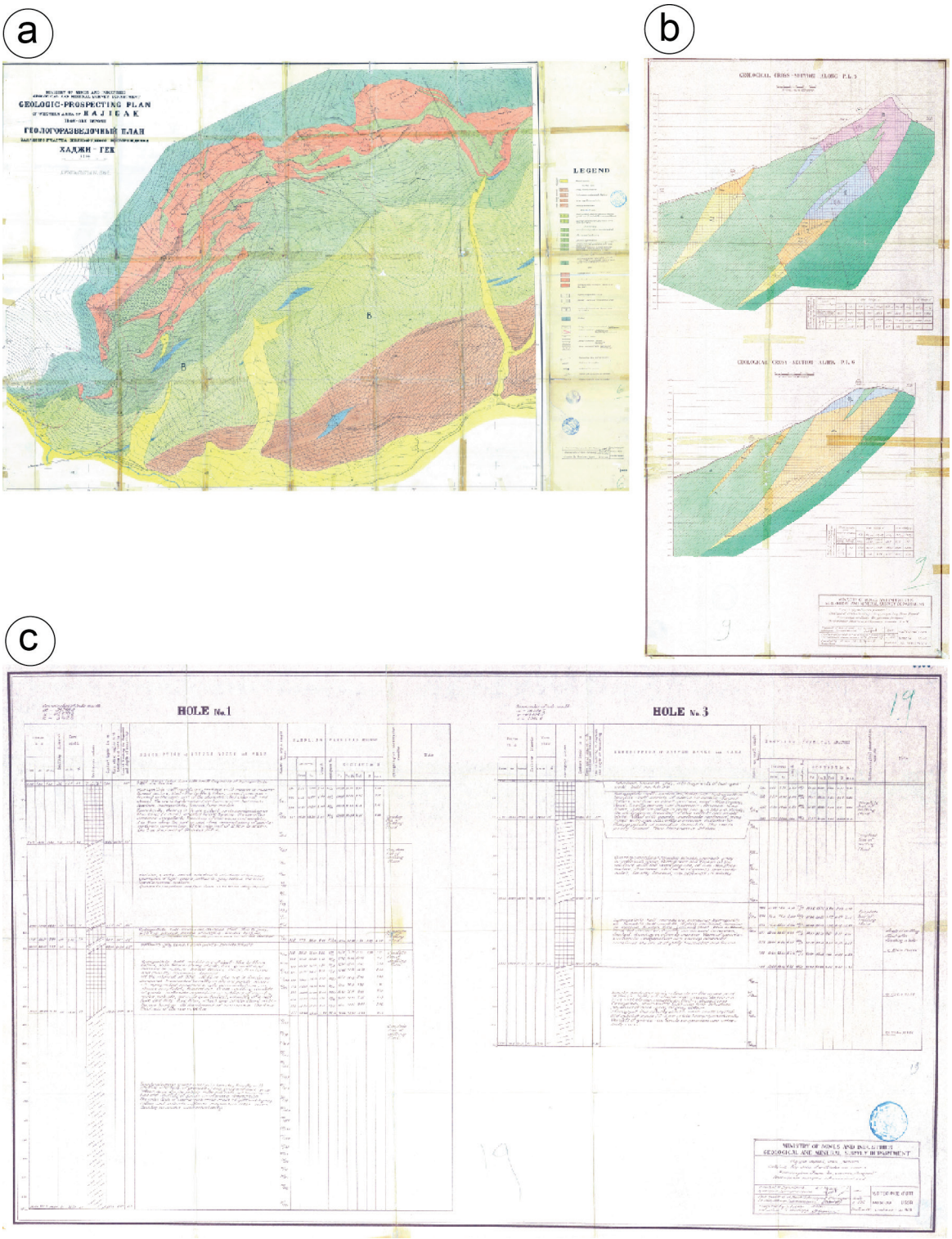

Figure 7A–3. Examples of illustrations from Soviet-era reports (Kusov and others, 1965a,b) on the Haji-Gak iron deposit. (*a*) Geologic prospecting plan of the western area of Haji-Gak; (*b*) Cross-sections used for calculations of ore reserves; and (*c*) Drill hole logs used for calculation of ore reserves. This scan is presented as an example of the style and type of study and reporting work that has been done in the past.

The main ore minerals within the sedimentary iron deposits in Afghanistan are hematite and magnetite and hematite, with smaller amounts of martite. The metallogenic age, mineralogy, textures, and sizes of the deposits make them compatible with several model types, such as Superior iron

deposits, Algoma iron deposits, and iron oxide copper-gold deposits. Sedimentary manganese deposits are a deposit type commonly associated with many sedimentary iron deposits throughout the world.

A permissive area for the occurrence of Haji-Gak-type iron deposits in Afghanistan was delineated by Peters and others (2007, p. 118–122) to encompass all Neoproterozoic sedimentary host rocks, which consist of greenschist facies schistose and phyllitic marble, dolomite, sandstone, and metavolcanic rocks (map unit Z_1scp) as well as associated Neoproterozoic metavolcanic andesite lava and interlayered sedimentary rocks (map unit Z_1al) (fig. 7A–4). Parts of the permissive tract outside the Haji-Gak iron area of interest are located in northern Kandahar, Zabul, Uruzgan, Ghazni, and Parwan Provinces (fig. 7A–4). A number of more favorable areas were also delineated to encompass the geology hosting deposits or occurrences like Haji-Gak (figs. 7A–5 and 7A–6). The updated favorable tract contains the Haji-Gak, Kharzar, Khaish, Chuy, Kharkiz, Darre-i-Neelee, and Zerak sedimentary-rock-hosted iron deposits (fig. 7A–6).

A southern part of the permissive area lies to the southwest of the Haji-Gak iron AOI and contains the Mangasak iron occurrence in Wardak Province and an unnamed stratabound manganese occurrence in northeastern Uruzgan province (fig. 7A–7). The Mangasak occurrence lies along the contact between Proterozoic gneiss and schist layers in a 1,200-meter (m)-long and 50- to -100-m-wide altered carbonated zone that contains magnetite as disseminations, nodules, and veinlets (Karapetov and others, 1970). The unnamed manganese occurrence consists of 1.5-m by 7-m lenses within Neoproterozoic cherty marl rocks (Abdullah and others, 1977).

Lack of unique and detailed descriptions of the Haji-Gak iron deposit at the time of assessment and questions concerning its genesis did not allow adequate model selection and this hampered the ability of the USGS Assessment Team in 2007 to make a quantitative assessment of the permissive area (Peters and others, 2007, p. 118–122). The main deposit types considered during the assessment process were Lake Superior-type iron deposits (Cannon, 1986a), Algoma iron deposits (Cannon, 1986b) and iron oxide copper-gold deposits (Cox, 1986; Haynes, 2000; Hitzman, 2000). After further study, the model that most closely resembles the Haji-Gak iron deposits is the Algoma iron type deposit, which is hosted by volcanogenic iron-bearing sequences mostly of Archean or Proterozoic age, similar to the Awband Formation at Haji-Gak. The Algoma iron type deposits form microbanded to mesobanded lenticular shapes that are less than 50 m thick and occasionally extend for more than 10 kilometers (km) along strike (Bekker, 2010), similar to the Haji-Gak iron deposit. Rock types that are associated with Algoma iron type deposits usually are mafic to felsic submarine volcanic rocks and deep-water clastic and volcanoclastic sediments. The textures of rocks in these iron deposits are pillowed greenstone, intermediate to felsic tuff and agglomerate, and poorly sorted clastic sediments (Cannon, 1986a,b). Individual volcanic rock layers are interbedded with deepwater greywacke and mudrocks.

7A.4 Known Deposits

The Haji-Gak iron AOI contains the Haji-Gak iron deposit (prospect subarea) in Bamyan Province and a number of other sedimentary rock-hosted deposits. Additionally there are several other deposits and prospects in the AOI and its subareas. The Haji-Gak iron deposit is the best known iron oxide deposit in Afghanistan, and similar occurrences of this type have been identified along a 600-km-long discontinuous east-west belt. The deposit is more than 12 km long and 3 km wide and contains 16 separate zones, some of which are up to 5 km long, 380 m wide, and extend 550 m downdip; seven of these zones have been studied in detail.

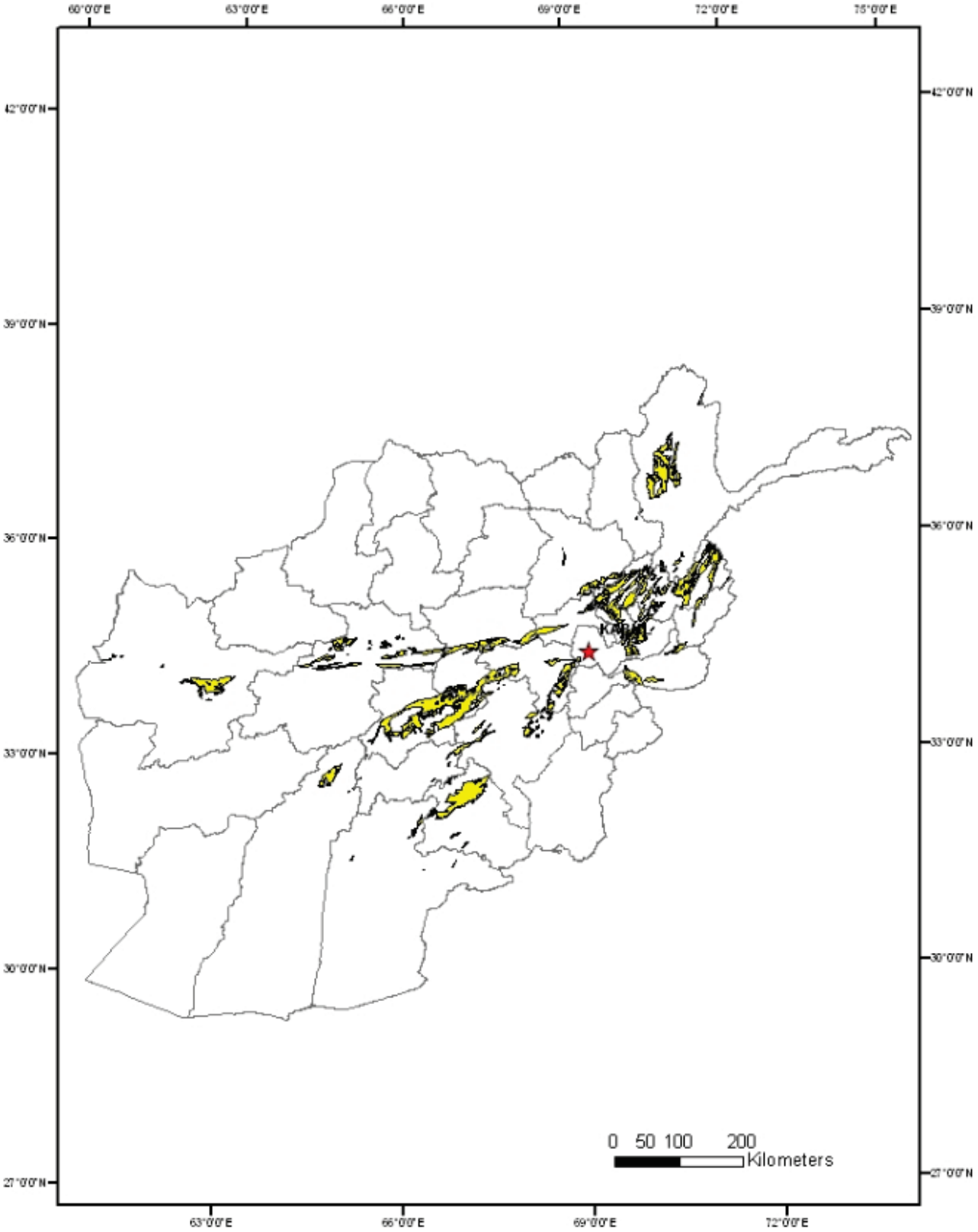

Figure 7A–4. Map of the Haji-Gak Neoproterozoic permissive tract sedFe-01 and the Paleoproterozoic permissive tract sedfe02 that contains undiscovered sedimentary-rock-hosted iron deposits, showing distribution of Proterozoic rocks that host the Haji-Gak iron deposit from Peters and others (2007). The red star is Kabul.

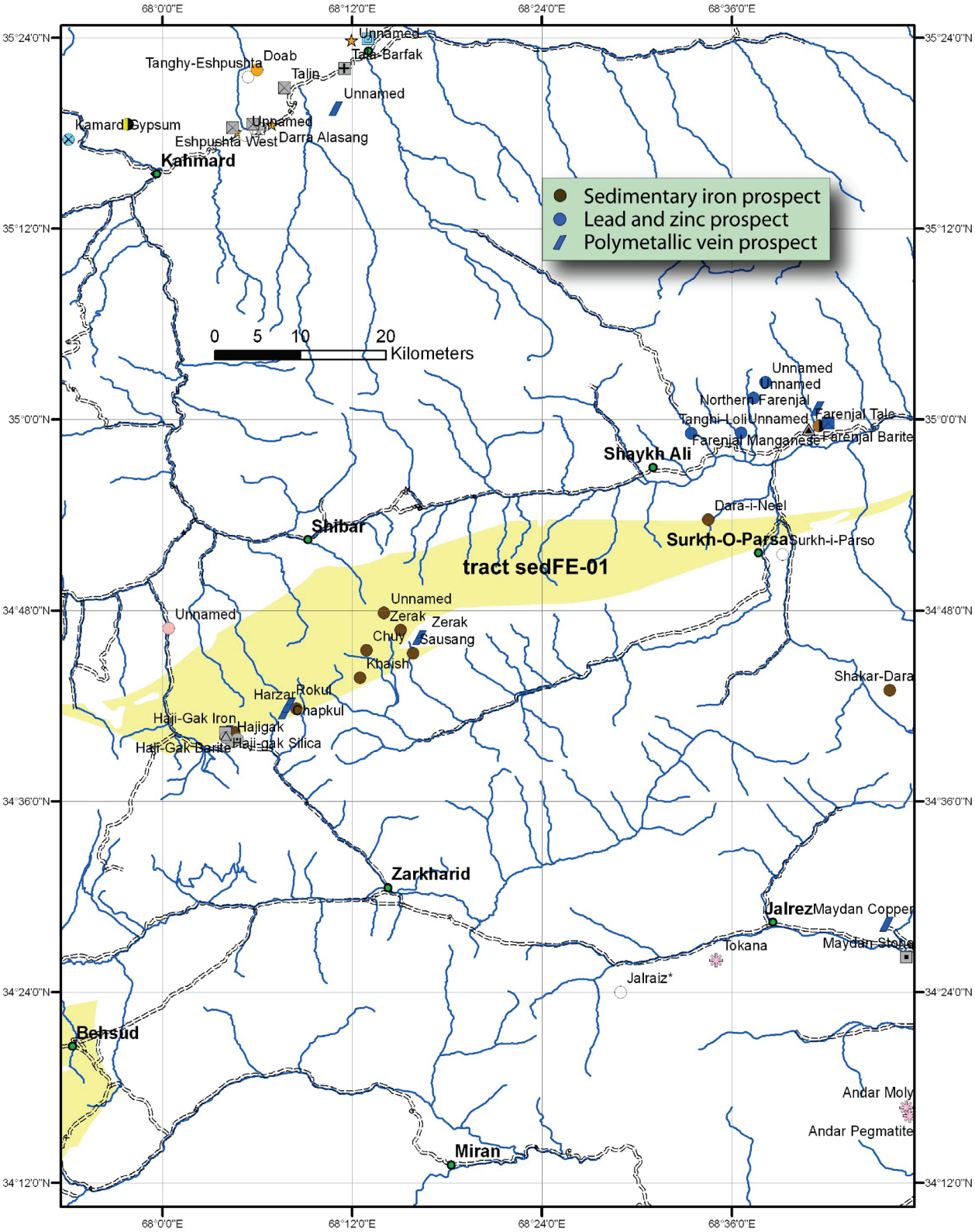

Figure 7A–5. Map showing parts of the permissive sedFe-01 Haji-Gak tract that contains the Haji-Gak and related deposits from Peters and others (2007).

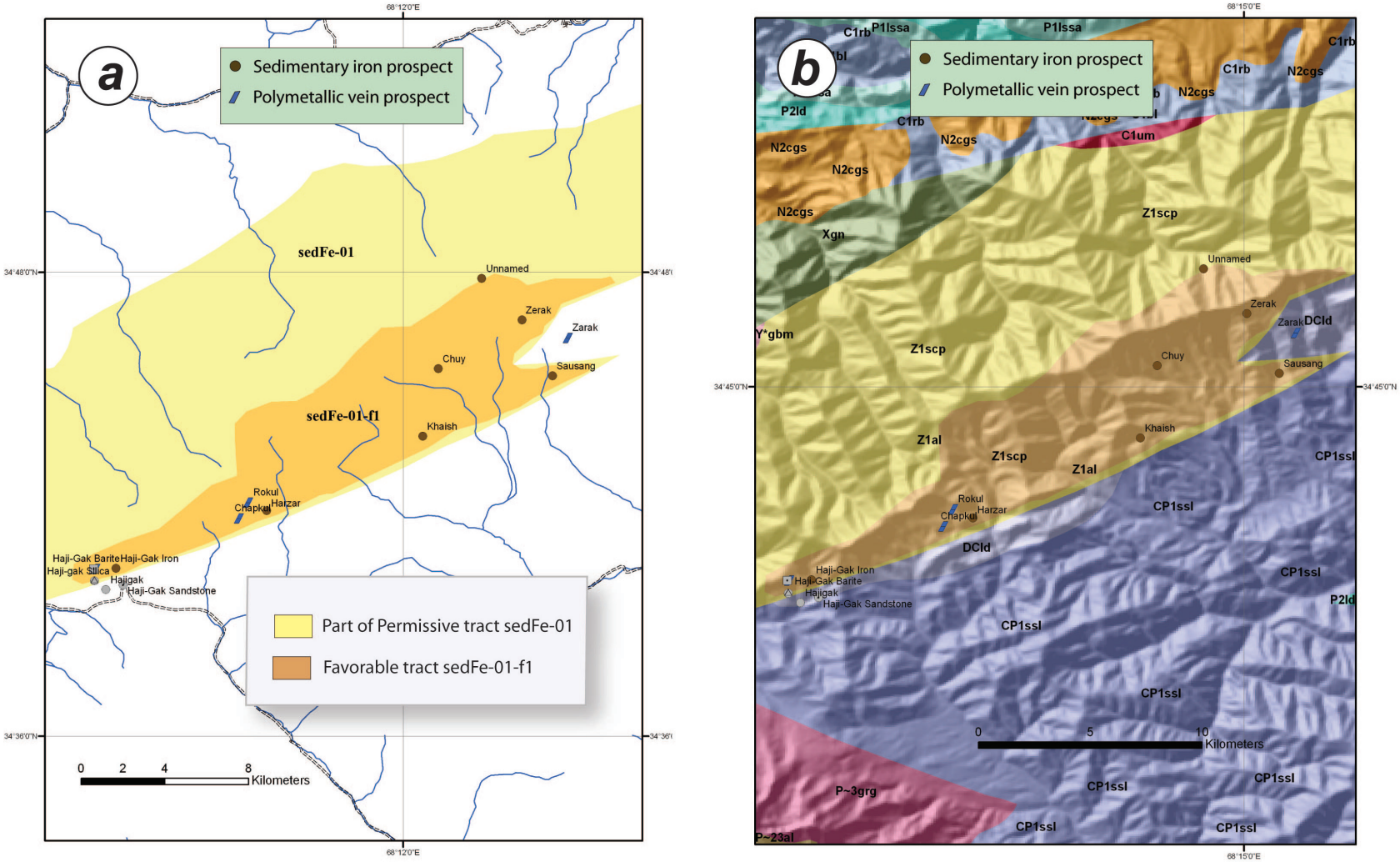

Figure 7A–6. Maps showing the location of the favorable sedFe-01-f1 Haji-Gak tract within larger permissive tract sedFe-01 tract from Peters and others (2007). (*a*) General location of favorable tract sedFe-01-f1. (*b*) Geologic units within and surrounding the Haji-Gak deposit. Host units within the tract consist of Z_1scp, Neoproterozoic greenschist, marble, dolomite, metavolcanic rocks including phyllite, schist, and sandstone; Z_1al, Neoproterozoic marble, dolomite, and metavolcanic rocks; DCld, Late Devonian to Mississippian limestone, dolomite, and schist;; and CP_1ssl , Carboniferous to Early Permian sandstone, siltstone, shale, and mafic volcanic rocks.

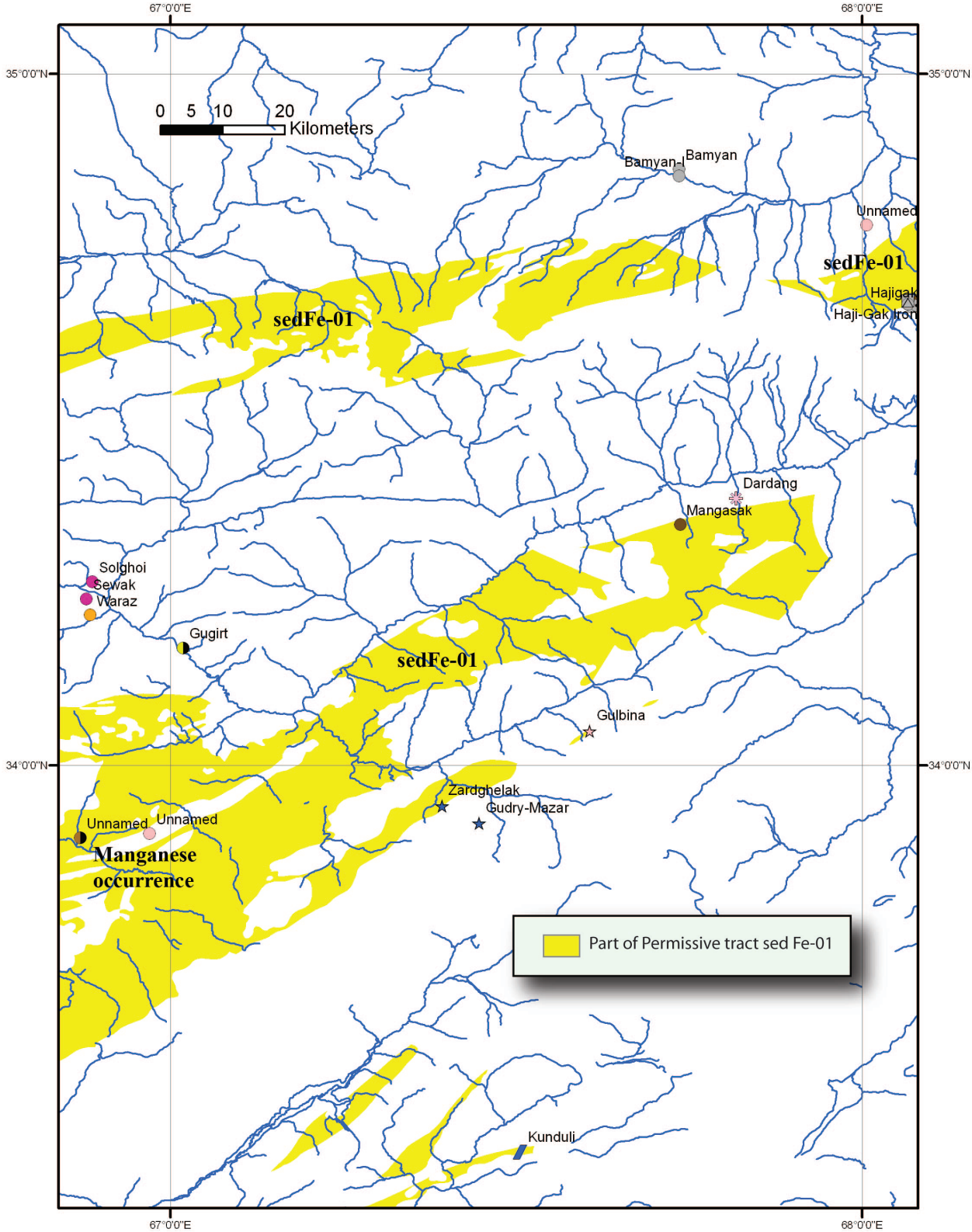

Figure 7A–7. Map showing southern parts of the permissivesedFe-01 Haji-Gak tract for undiscovered sedimentary iron deposits from Peters and others (2007). The southern parts of the tract contain the Mangasak iron occurrence and a stratabound unnamed manganese deposit to the southwest.

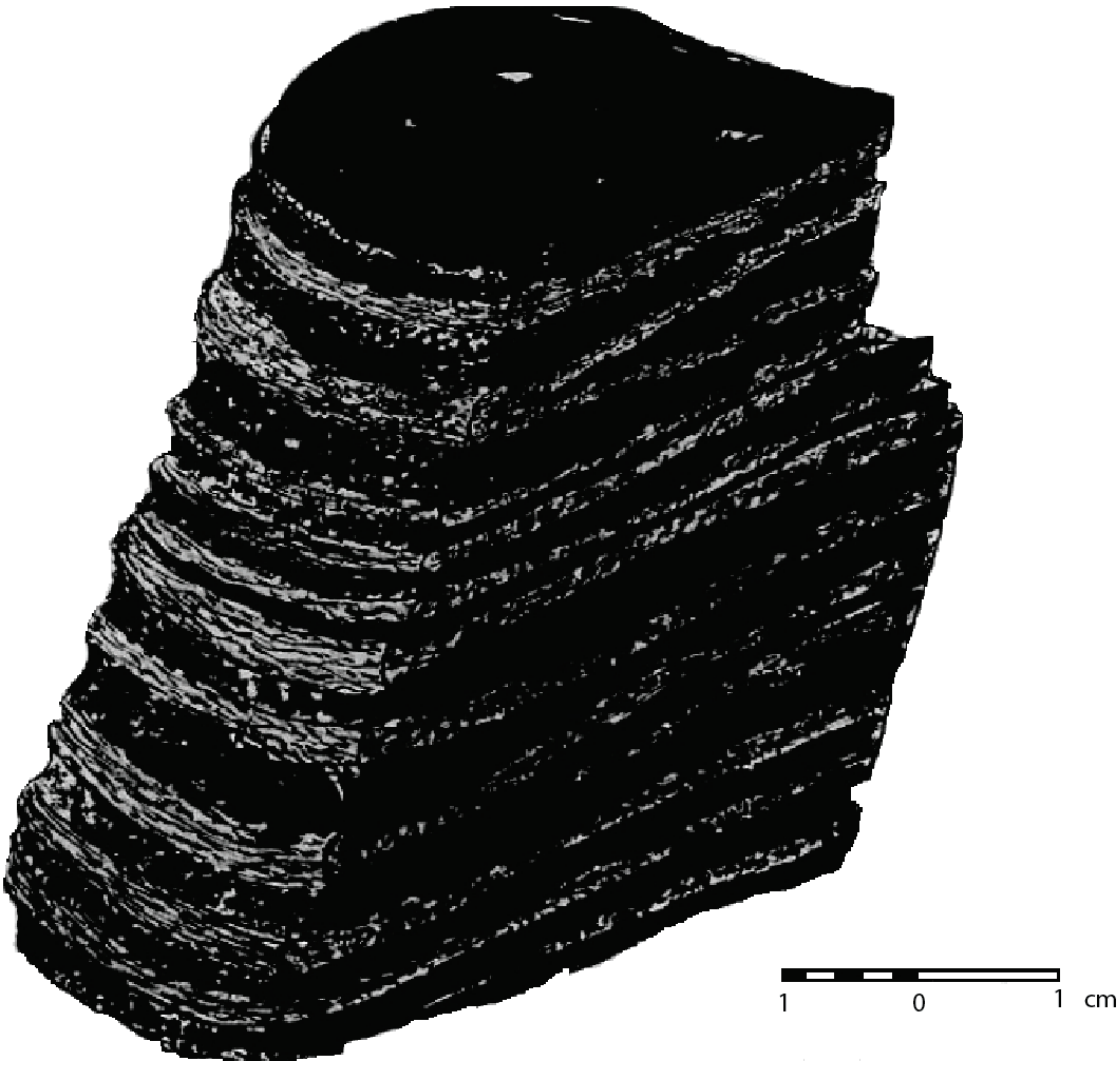

Figure 7A–8. Photograph of a banded hydrogoethite-hematite-semimartite. The light bands are made of hematite, and the black bands are made of magnetite, martite, and hydroxides. The sample in the photograph is from drill hole # 2 at a depth of 36.30 meters (Kusov and others, 1965a,b).

Iron ore is both primary and semioxide. The primary ore [80 volume percent (vol. %) of the deposit] is present below 130 m and comprises magnetite, pyrite, and minor other sulfide minerals, including chalcopyrite, and averages 61.3 weight percent (wt. %) iron. The remaining 20 vol. % of the ore is oxidized and consists of three hematitic ore types at slightly higher grades than the primary ore. The mineralization is structurally controlled. Previous Russian resource estimates for the entire deposit are 1,700 million metric tons (Mt), although the mining reserve estimate for the near-surface oxide ore in the most explored area is 85 Mt (table 7A–1; Momji and Chaikin, 1960; Mirzad, 1961; Kusov, 1963; Kusov and others, 1965a,b; Bouladon and de Lapparent1975; Abdullah and others, 1977).

The Haji-Gak orebody no. 1 extends 5 km, the strike of the deposit is southeasterly at 140° to 150º with a dip angle of 60° to 70º, and is 110 m thick. The Haji-Gak iron orebodies cover an area of 35 km^2. There are six drill holes, two adits and three reserves of about 20 Mt of ore (table 7A–1). The deposit was discovered in 1911 by G.T. Hyden of the Indian Geological Survey. The mineral composition of the Haji-Gak orebody no. 1 is 30 vol. % magnetite, 25 vol. % hydroxides, 20 vol. % martite, 7 vol. % quartz, and 5 vol. % hematite (Sutphin and others, 2010).

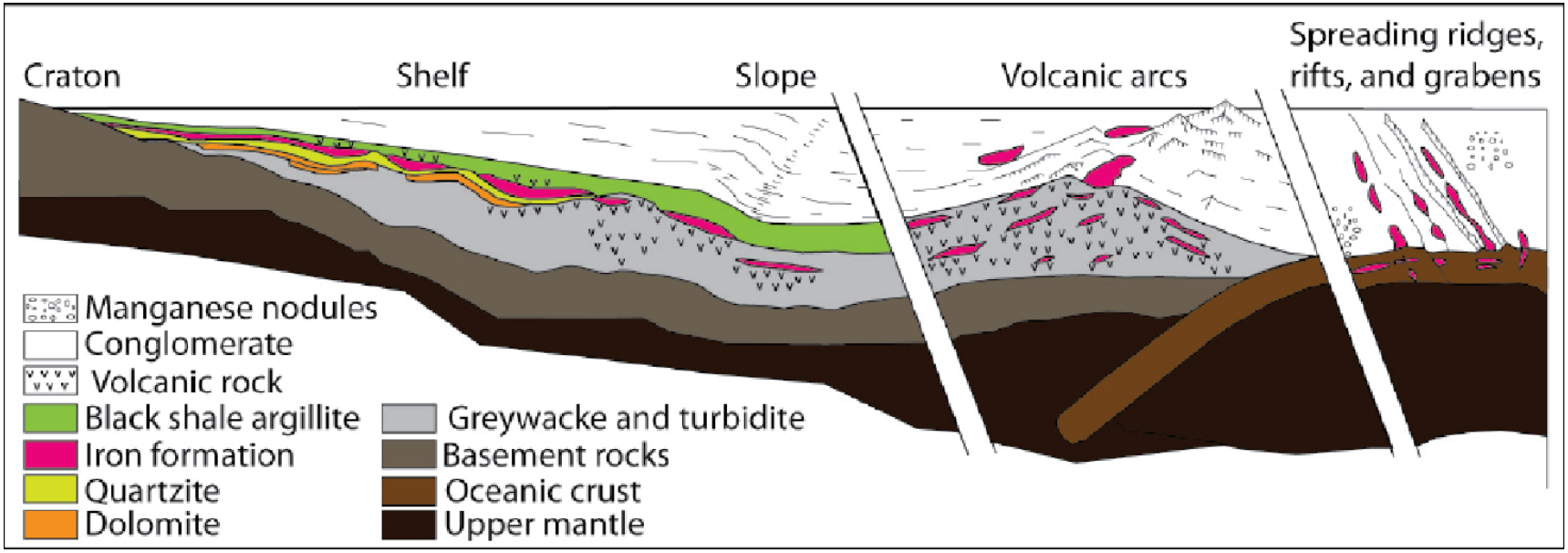

Figure 7A–9. Diagram of the environment most likely for the formation of sedimentary and volcanogenic iron deposits. The diagram shows the formation of Algoma iron type deposits near the Volcanic arc and Lake Superior type deposits near the upper shelf. Rocks of each type of deposit are represented. The Haji-Gak iron deposit contains rocks more closely related to volcanoclastic settings. Diagram modified from Gross (1973) and Peters (2010).

7A.5 Geology of the Haji-Gak Iron Deposit Area

The 1:1,000,000-scale geologic map of Doebrich and Wahl (2006) shows the Haji-Gak iron deposit to be hosted in Neoproterozoic sedimentary rocks, which are described as greenschist facies schistose and phyllitic marble, dolomite, sandstone, and metavolcanic rocks (map unit Z_1scp). The deposit is also interbedded with Neoproterozoic metavolcanic andesite lava and interlayered sedimentary rocks (map unit Z_1al).

The oldest part of the Haji-Gak Proterozoic stratigraphic succession, as described by Kusov and others (1965a,b), is the Neoproterozoic Kab Formation that contains quartz-sericite schist, phyllite, marble, and dolomite and porphyrite lenses (fig.7A–11). The Haji-Gak iron deposit is hosted by the Neoproterozoic Awband Formation, which, together with the underlying Kab Formation, forms the 4,500-m-thick Qala Group, a sequence of metavolcanic and metasedimentary rocks that comprise tuff, argillaceous rocks, and minor chert and marble. The Awband Formation comprises sericite and quartz-sericite schist, sandy quartz sericite schist, carbonate chlorite-sericite schist, marble, dolostone, and plagioporphyrite with scapolite, volcanic rocks, and tuff. The iron orebodies in the Neoproterozoic Awband Formation are overlain by the Green Schist Formation (fig. 7A–11) that is dominated by quartz-chlorite-sericite schist and quartz-chlorite schist, plagioporphyrite with scarce scapolite, and metavolcanic rocks that locally are intruded by granodiorite (figs. 7A–12, 7A–13, and 7A–14).

Intrusive complexes are present in the Proterozoic rocks of Haji-Gak iron deposit area. The oldest consists of small intrusions of quartz porphyry, plagiogranite, and quartz diorite, including granodiorite. The youngest includes sills, dikes, and small stocks of diabase. In addition, there are local occurrences of keratophyre and metasomatic carbonatite. Serpentine bodies also are present and comprise thin (up to 5-m) sills and dikes with microflaky and spotted textures. The serpentine rocks are green, schistose, and fine-grained. The primary mineralogy of the serpentine rock has been converted to secondary antigorite, talc, and magnesite as well as later minerals, such as brucite and carbonate, that are mostly developed in the Jowqul Formation and more rarely in the Kharzar Formation.

These Paleoproterozoic volcanoclastic rocks are unconformably overlain by the Upper Devonian Haji-Gak Formation that contains remnants of corals and brachiopods and comprises grey-black limestone injected with a thick network of white, coarse-crystalline barite veins, calcareous conglomerate and breccias, calcareous-clayey shale, sandy limestones, calcareous sandstones, and quartzite (figs. 7A–11 and 7A–15). The Lower Carboniferous Kharzar Formation unconformably overlies the Haji-Gak Formation and contains shale, sandstone, and quartzite. These formations are as thick as 500 to 900 m.

The Quaternary rocks are Holocene to Recent floodplain and fluvial, alluvial-colluvial, and fluvioglacial moraine deposits and glacial outwash. The deposits of fragmental iron ore are located in Recent colluvial deposits (figs. 7A–11 and 7A–15).

The Haji-Gak iron orebody and its host rocks are folded and faulted (fig. 7A–15). The predominant strike of the Proterozoic and Paleozoic rocks is between northeast and north-northeast, with a regional dip of approximately 50° towards the south-southeast or southeast and a general plunge of mesoscopic and macroscopic folding to the southeast (fig. 7A–16*a*,*b*). Strikes and dips of bedding and bedding plane parallel foliation were compiled in the study in 11 separate structural domains in the main Haji-Gak iron deposit area from the maps of Kusov and others (1965a,b) and these data were plotted as poles to planes and then contoured on equal area stereonets (fig. 7A–16*a*). Strikes of the fold axial planes were identified from inferred folding of the ore on the map, and dips of the axial planes were approximated from the stereonet plots. The results of this analysis confirmed that the dominant plunge of folds in the host rocks and the contained ores is about 40° to 50° southeast (fig. 7A–16*a*).

One major steeply dipping fault has juxtaposed the Neoproterozoic rocks against the crystalline Mesoproterozoic rocks (fig. 7A–15). Another fault has thrown Upper Devonian rocks against the Neoproterozoic Green Schist Formation. In addition, a number of north-south and north-west trending faults, some of which are probably thrusts, offset parts of the Neoproterozoic succession, including the

iron ore deposits. A series of thrust faults have been mapped by Kusov and others (1965a,b) and are also indicated by the increased thickness of the iron ore and its host rocks within the central zone of the Haji-Gak iron orebody. A final phase of faulting consisted of the development of north-south and northwest-southeast faults that have offset the iron ores. Later post-Cretaceous extension led to the further development of northwest-southeast faults and graben structures that are filled with Quaternary to Recent sediment.

Figure 7A–10. Photograph of the Haji-Gak iron deposit looking northeast. The dark-colored outcrops (indicated by arrows) along the ridge line are the outcropping parts of the Haji-Gak iron orebody. Photograph by Will Stettner, U.S. Geological Survey.

Zones of contact metamorphism contain breccia zones near the orebodies that are dense and massive and contain local relict bedding. These breccia zones are highly fragmented and have micrometagranoblastic and microgranoblastic textures. These zones comprise quartz, iron hydroxide minerals, hydromica, and sericite, as well as local zoisite. Microquartz is common in many of the volcanic rocks, and mylonitization zones also are present as lenses of mylonitized and brecciated limestone that are up to 5 m thick along the base of plagioporphyrite and quartz plagioporphyrite in the Green Schist Formation.

7A.6 Structural Geology

The rocks of the Haji-Gak iron ore deposit form a large horizontally extended monocline, which coincides with the south limb of the larger Khoh-e-Baba anticlinorium. The rocks strike northeast and dip southeast (azimuth from 120° to 170°, angle from 35° to 80°). The monocline also contains smaller folds and fractures. The orebodies are conformable with layering of the host rocks. The Haji-Gak iron ore field has been divided into three northeast structural zones by Kusov and others (1965b)—the northern, middle, and southern zones.

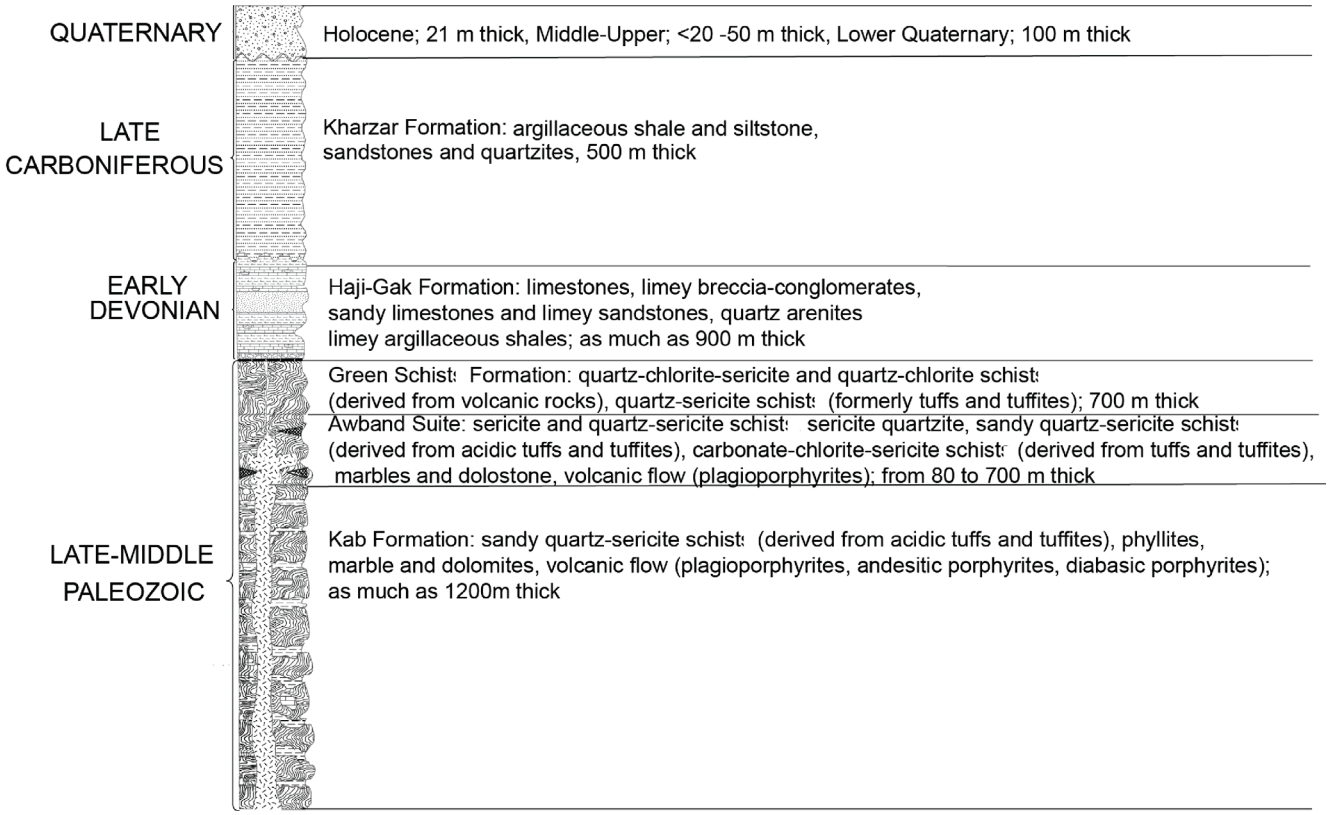

Figure 7A–11. Stratigraphic column of the Haji-Gak iron deposit area. Drafted from data from Kusov and others (1965b).

The northern structure zone contains cyclically repeated interbedded layers of schist with fine- to medium-textured phyllite as well as local interlayers of siliceous limestone (Kab Formation).Formation This zone is monoclinal and contains southeast dips (azimuth from 110° to 170°, dip angle from 35° to 60°). In addition, this zone contains small-scale isoclinal, locally recumbent folds. Faults in the northern structure zone are brittle, but flow cleavage and shear zones are parallel to the schistocity.

The middle structural zone consists of the Awband and Green Schist Formations. The northern border of this zone coincides with the contact between the Awband and Kab Formations, and orebodies I, IX, and XII are located along this locally faulted contact. The southern contact of the middle structural zone passes along the Haji-Gak-Kharzar Fault. This zone comprises rocks having contrasting physical characteristics, including iron ore, various schists, sericite quartzite, marble, volcanic rocks, and alkaline rocks. These mixed physical properties played a major role in intense dislocation in this section compared with that of other sections. The middle structural zone is also monoclinal with the steep southeast dips (50° to 80° southeast). Most secondary folding in the Haji-Gak iron district is present in this zone. There are small symmetric and asymmetric folds, overturned and recumbent with limbs with dip lengths that range from 20 to 200 m and extend along strike for between 200 and 600 m. Kink banding is present within the schist. The faulting in the middle structural zone is both mesoscopic and megascopic, and cleavage is well developed. Foliation and shearing are abundant in the middle structural zone, as are brittle faults. The iron orebodies are fractured parallel to cleavage. The banded ore is sheared and marked by flow cleavage parallel to the schistocity.

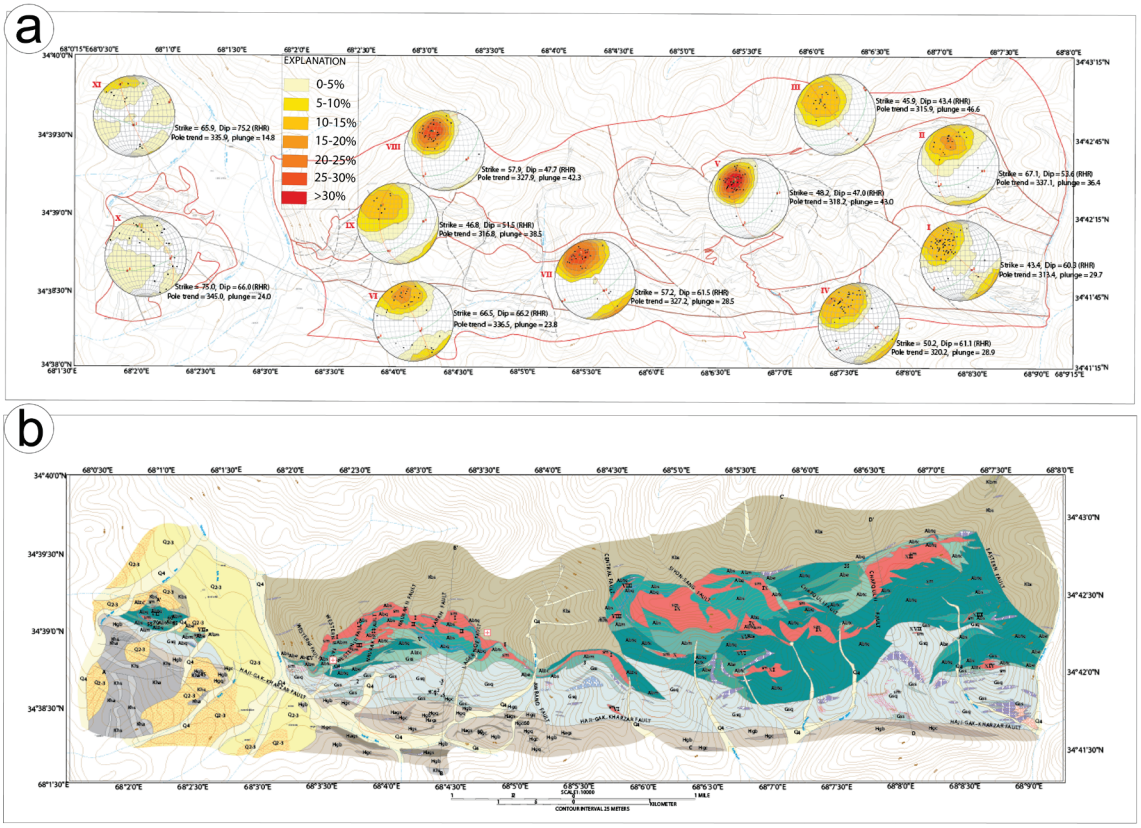

Q4 Flood-plain and alluvium deposits (HOLOCENE)
Eluvium-diluvium deposits (colluvium) (HOLOCENE)

Q2-3 Morainal deposits (QUATERNARY)

Q2-3 Glacio-fluvial drift (QUATERNARY)

KHARZAR FORMATION (LOWER CARBONIFEROUS)

Khs Sandstones and Quartzites sandstones

Kha Argillaceous shale and siltstones

HAJI-GAK FORMATION (UPPER DEVONIAN)

Hgb Grey limestone

Hgc Limey breccia-conglomerates

Hags Sandy limestones and limey sandstones

Hgq Quartz Sandstone

Hgs Limey argillaceous shales

GREEN SCHIST FORMATION (LOWER-MIDDLE PALEOZOIC)

Gsq Quartz-chlorite-sericite and quartz-chlorite schist (derived from volcanic rocks)

Gss Quartz-sericite schist (formerly tuffs and tuffites)

AWBAND FORMATION (LOWER-MIDDLE PALEOZOIC)

Abs Sericite and quartz-sericite schist

Abq Sericite quartzite

Abtq Sandy quartz-sericite schist (derived from acidic tuffs and tuffites)

sm Semi-oxidized hydrogoethite-semi-martite ore

gh Semi-oxidized carbonate-semi-martite ore

mm Semi-oxidized hydrogoethite-hematite-semi-martite

Non-oxidized pyrite-magnetite ore, carbonate-magnetite ore-pattern shown in core holes only

Abtc Carbonates-chlorite-sericite schist (derived from tuffs and tuffites)

Abm Dolomitic marbles

KAB FORMATION (LOWER-MIDDLE PALEOZOIC)

Kbs Sandy quartz-sericite schist and phyllites (derived from tuffs and tuffites) fragments

Kbm Marble and Dolomites

Kbe Volcanic Flow

INTRUSIVE ROCKS

Diabase

Figure 7A–12. Structural analysis of bedding and foliation of the Haji-Gak iron orebody from Renaud and others (2011a). *(a)* Contoured poles to bedding on equal area stereonets from 11 separate domains showing moderate plunges to the southeast. (*b*) Geologic map of the Haji-Gak iron ore deposit.

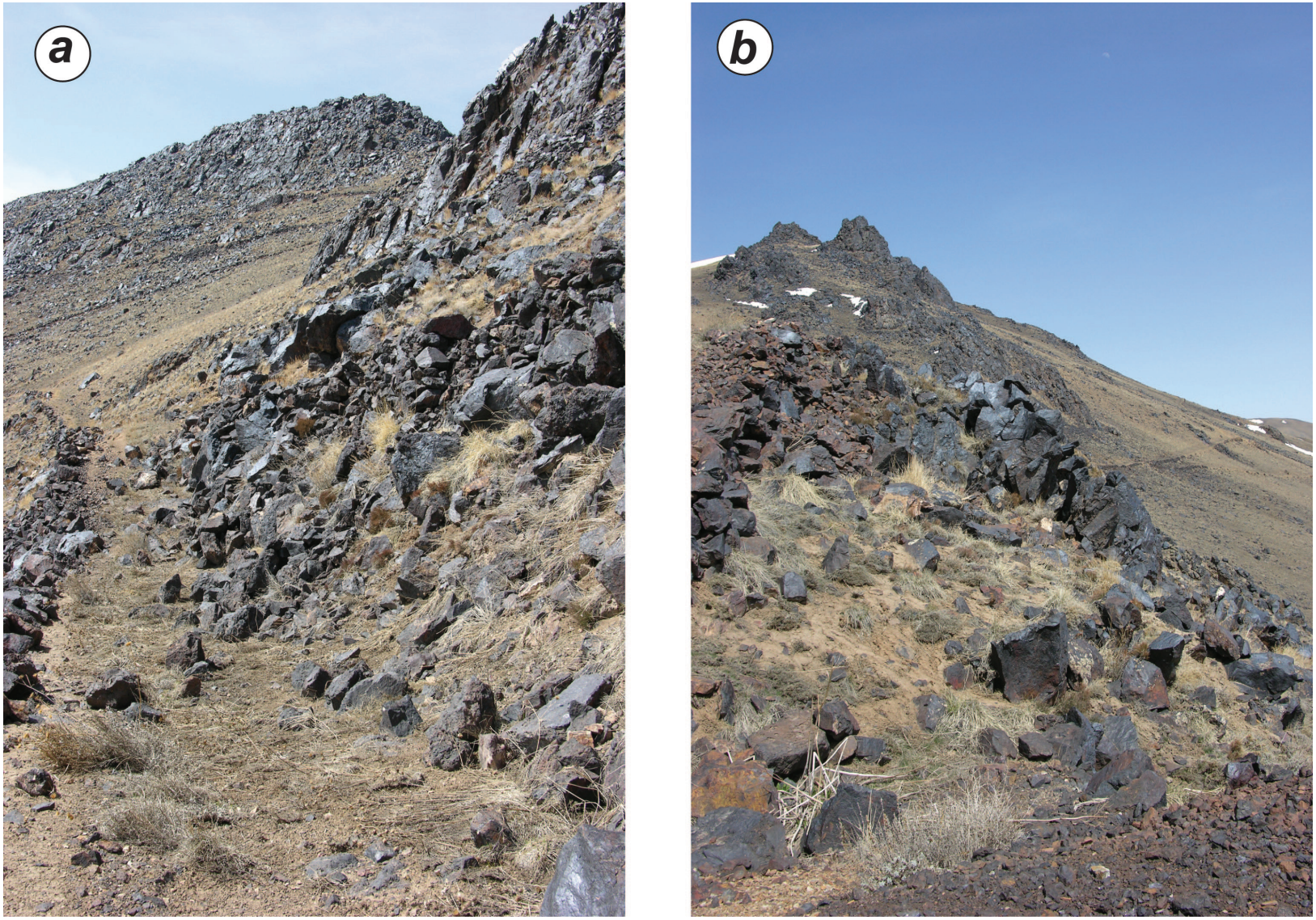

Figure 7A–13. Photographs of outcrops of the Haji-Gak sedimentary iron deposit in Bamyan and Wardak Provinces from Peters and others (2007). (*a*) Pathway along outcrops of iron ore. (*b*) Outcropping layers of iron ore along the crest of the main ridge at Haji-Gak. Photographs by Robert Bohannon, U.S. Geological Survey.

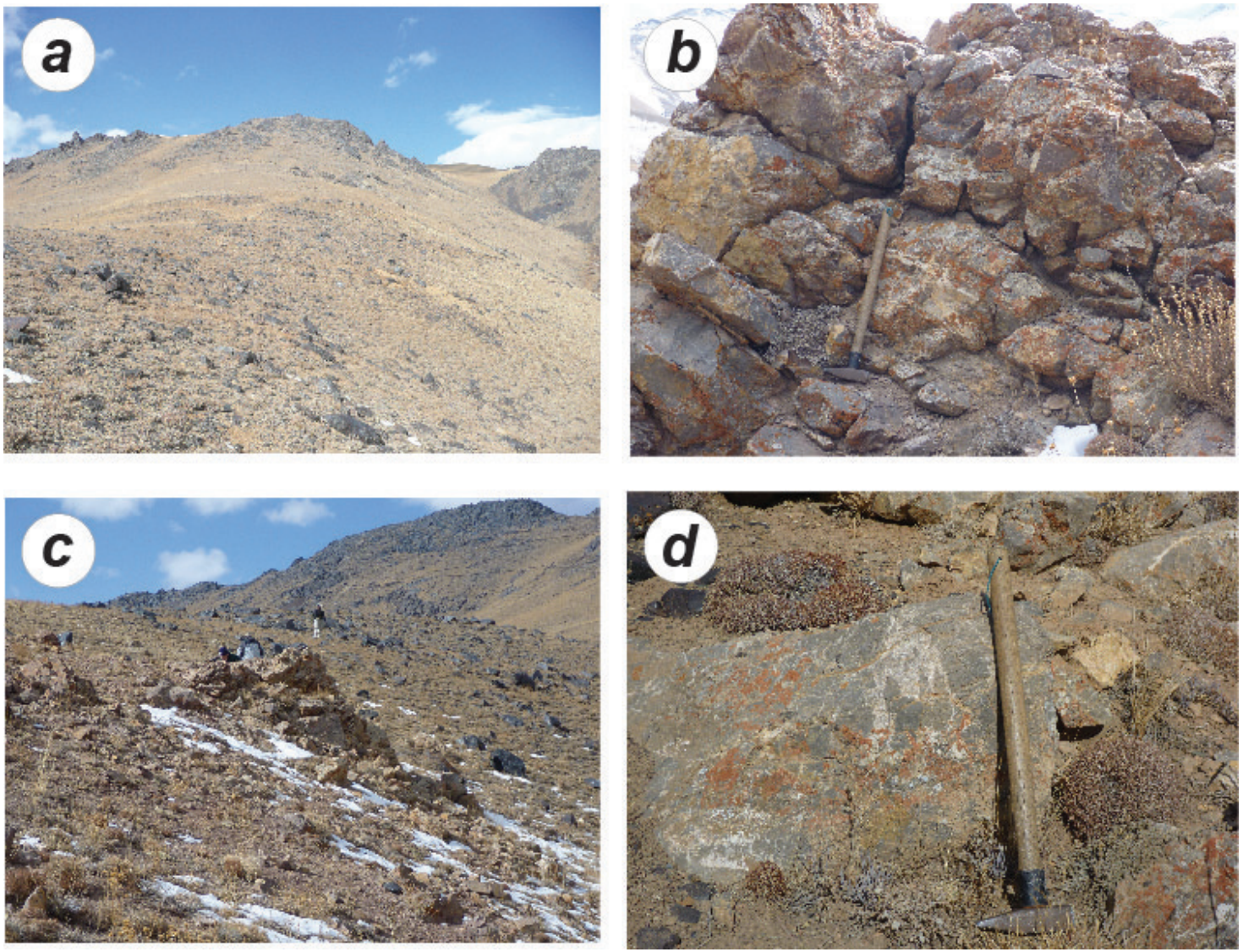

Figure 7A–14. Photographs of the Haji-Gak iron deposit area. (*a*) North view of the massive magnetite deposit at Haji-Gak (Stop 2, 34.66288° N, 68.06736° E). (*b*) Close-up of south-dipping fine-grained bedded and brecciated limestone at the contact with massive magnetite (GPS 34.66299° N, 68.06770° E). (*c*) View looking NW of the contact between massive magnetite (right, north) and fine-grained limestone (west, south). (*d*) Close-up of limestone showing the brecciated character and small clusters of magnetite (black) within the breccia matrix. Photographs by Robert D. Tucker, U.S. Geological Survey.

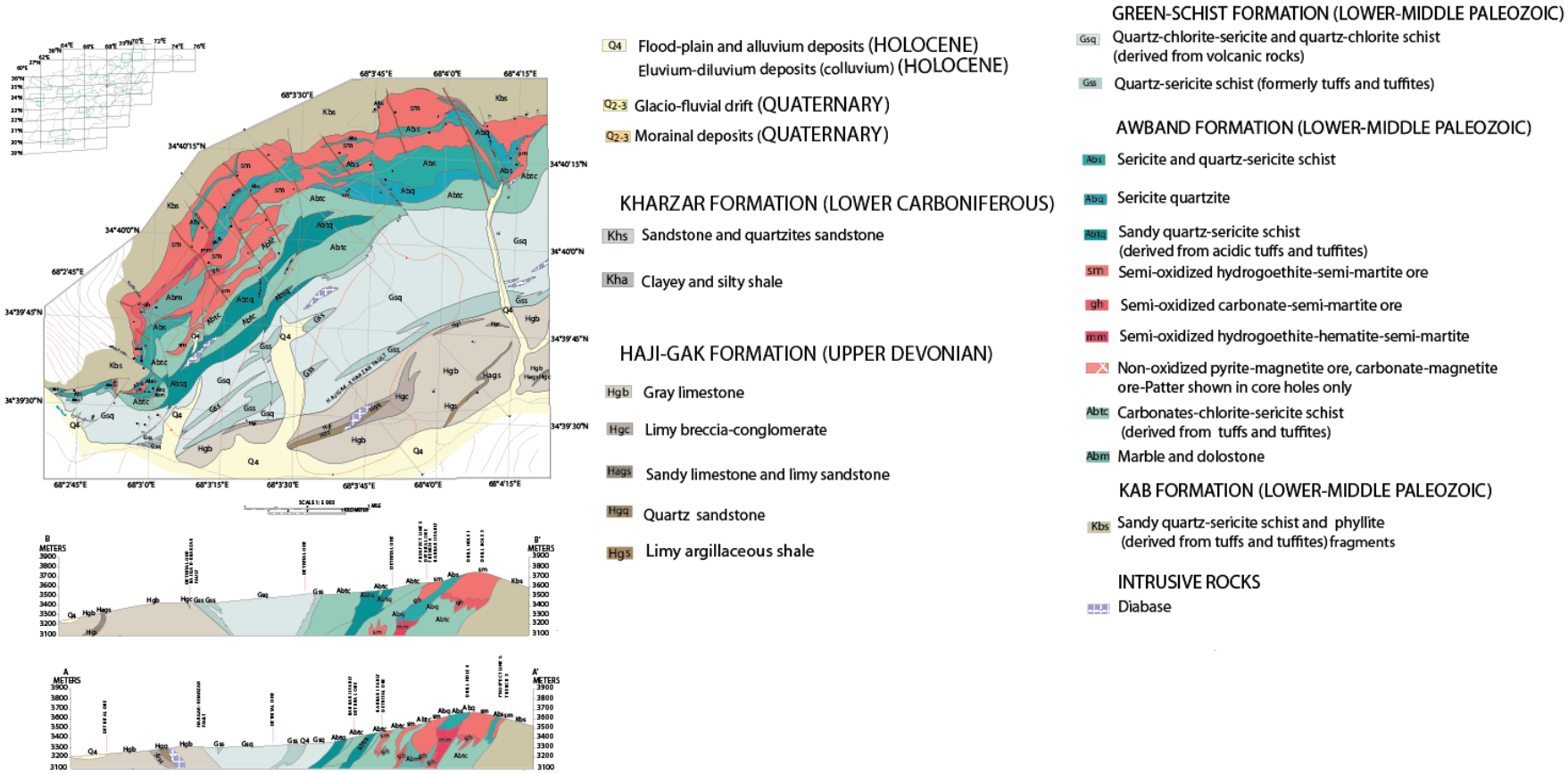

Figure 7A–15. Geology and cross-sections of the western parts of the Haji-Gak main iron orebody, modified from Kusov and others (1965a).

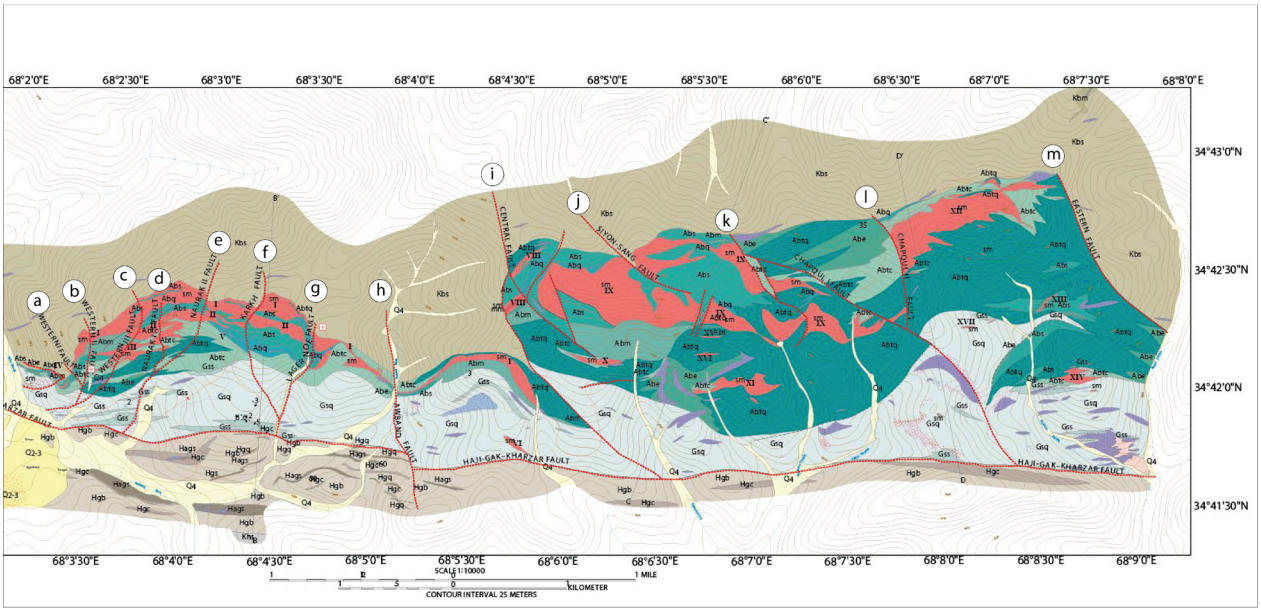

Q4 Flood-plain and alluvium deposits (HOLOCENE)
Eluvium-diluvium deposits (colluvium)(HOLOCENE)

Q2-3 Morainal deposits (QUATERNARY)

Q2-3 Glacio-fluvial drift (QUATERNARY)

KHARZAR FORMATION (LOWER CARBONIFEROUS)

Khs Sandstone and quartzites sandstone

Kha Clayey silty shale

HAJI-GAK FORMATION (UPPER DEVONIAN)

Hgb Gray limestone

Hgc Limy breccia-conglomerate

Hags Sandy limestone and limy sandstone

Hgq Quartz sandstone

Hgs Limy argillaceous shale

GREEN SCHIST FORMATION (LOWER-MIDDLE PALEOZOIC)

Gsq Quartz-chlorite-sericite and quartz-chlorite schist (derived from volcanic rocks)

Gss Quartz-sericite schist (formerly tuffs and tuffites)

AWBAND FORMATION (LOWER-MIDDLE PALEOZOIC)

Abs Sericite and quartz-sericite schist

Abq Sericite quartzite

Abtq Sandy quartz-sericite schist (derived from acidic tuffs and tuffites)

sm Semi-oxidized hydrogoethite-semi-martite ore

gh Semi-oxidized carbonate-semi-martite ore

mm Semi-oxidized hydrogoethite-hematite-semi-martite

Non-oxidized pyrite-magnetite ore, carbonate-magnetite ore-pattern shown in core holes only

Abtc Carbonates-chlorite-sericite schist (derived from tuffs and tuffites)

Abm Marble and dolostone

KAB FORMATION (LOWER-MIDDLE PALEOZOIC)

Kbs Sandy quartz-sericite schist and phyllite (derived from tuffs and tuffites) fragments

Kbm Marble and Dolomite

Kbe Volcanic Flow

INTRUSIVE ROCKS

Diabase

Figure 7A–16. Geologic map showing faults described in this chapter of this report and listed in table 7A–1 (indicated by letters in circles). From Renaud and others (2011a).

The southern structural zone is confined to the Haji-Gak Formation. These rocks are deformed, especially near faults, but not as deformed as the rocks in the middle structural zone. Overturned folds are prominent near the Haji-Gak-Kharzar Fault. The carbonated rocks of this zone were fractured and contain horsetail fractures. Rocks near cross faults dip to the northwest (azimuth from 315° to 340°,

angle from 80° to 90°), but movement is scissor-like because, along the southern part of the cross-fault, the dip of the rock changes to the southwest with an azimuth of 130° to 160° and angles of 50° to 70°.

Kharzar Formation rocks are located to the south of the southern section. This flyschoid unit comprises clayey and sandy schists with interlayers of sandstones and microquartz. This unit has a monoclinal dip to the southeast and angles from 40° to 70° with weak secondary folding.

Faults in the Haji-Gak iron ore deposit field are transverse and diagonal and occasionally parallel to the bedding and schistocity. The size and movement of the faults varies from large to small strike-slip or dip-slip faults, thrust faults, and normal faults and shear zones along the cleavage. The biggest fault in this area is Haji-Gak-Kharzar followed by the following transverse and diagonal faults (listed by direction from west to east): Western I, II, and III, Naurak I and II, Khark, Lagernoye, Awband, Central, Sio-Sang, Chapkul I and II, and Eastern (fig. 7A–16; table 7A–22).

The Haji-Gak-Kharzar Fault extends 32 km along strike on a northeast bearing throughout the entire orebody and beyond (fig. 7A–16; table 7A–13). The Haji-Gak-Kharzar Fault is a thrust fault with displacement amplitude of between 700 and 1,000 m. Green Schist Formation rocks have been thrusted on top of the Haji-Gak rocks. On the surface, the Haji-Gak-Kharzar Fault displays an irregular 3-to15-m-high fault scarp. Rocks along the fault are characterized by ductile deformation, fault rocks containing clay, and many slickensides on both walls of the fault. Schist and volcanic rocks near the fault are closely folded and mylonitized (fig. 7A–17).

Other major faults are the Western, Naurak, Kharh, Lagernoye, Awband, Central, Sio-Sang, Chapkul, and Eastern Faults (fig 7A–16; table 7A–2).) These faults are irregular transverse and diagonal and locally pass into horsetail morphology. The faults are left- or right-lateral or thrust faults, which offset the iron orebodies into blocks and displace them into steps or horsts and grabens (fig. 7A–16). These faults are brittle faults, having displacements of between 20 to 120 m horizontally and from 10 to 50 m vertically. Along the Central Fault, the displacement is up to 1,400 m.

Slickensides, streaks, and furrows are common along on the surfaces of displaced blocks along the fault boundaries. Most of these fault structures are diagonally oriented between 40° and 50°. Some of the faults (Naurak, Western II, Central, and Chapkul) contain 2- to 10-m-wide fracture zones (fig. 7A–16; table 7A–2).

The faults with the largest displacements are the Central and Chapkul II Faults, which break the iron ore field into three large blocks (fig. 7A–16; table 7A–2). Kusov and others (1965a) indicated that these faults predate the iron ore formation but that the orebodies in the three blocks were further broken into smaller blocks.

Lesser faults have formed in the ore. These are small faults that usually are splays of the larger faults. Normal faults are present in orebodies, on their contacts and in the host rocks. The displacement varies from 1 to a few meters mostly and in places can reach up to 10 m10

Dikes and volcanic rock veins; quartz, barite, and calcite veinlets; and small hematite-magnetite ore veinlets are abundant in the Awband Formation host rocks and in the Green Schist Formation ore in the exocontact section of orebodies in the Kab Formation. These structures are mainly conformable and in places cross-cutting. Dikes are penetrated by hematite-magnetite ore veinlets. A few orebodies contain quartz veinlets and, in parts, quartz-carbonate and hematite veinlets. Orebodies in places do not have conformable contacts with the host rocks.

Kusov and others (1965b) suggest that much faulting occurred before ore formation, but that fractures and cleavage structures are present in all the orebodies and in all rocks that constitute the ore field.

There are four joint fracture systems according to Kusov and others (1965b). Most of joints strike northwest, as follows:

- azimuth dip from 175° to 215°, angle from 20° to 80°
- azimuth dip from 5° to 75°, angle from 70° to 90°
- azimuth dip from 115°to 155°, angle from 40° to 90°
- azimuth dip from 320°to 335°, angle from 80° to 90°

In places, foliation has the same attitude as the banding in iron ores, which is compatible with a volcanogenic origin for the ores. This similarity in attitude would imply that most of the faulting postdated the formation of the iron ores. However, there are indications that faults predated the formation of the iron ore in an epigenetic setting according to Kusov and others (1965b). These indications include the following:

- abundance of diabase dikes, which are conformable and in some places cutting (with cross-cutting veinlets, and in some parts with ore impregnations)
- the presence of small veinlets of ores, such as quartz-hematite-magnetite, quartz-magnetite and hematite-magnetite in Awband Formation schist
- the presence of parallel ore veinlets in diabase dikes along the contact of orebodies VII and IX
- filling the cutting contacts of host rocks by orebody materials with veinlets dispersion near salbands in host rocks
- the presence of brecciated structures in the iron ores, indicating the pre-ore fracture of marbles, derived from the Central and Chapkul II Faults as well as other faults

Small fractures in the iron ores owing to deformation show the same content as the primary content of orebodies. It is possible that some of these fractures formed by quartz-carbonate or quartz-carbonate-barite veinlets, which appear in orebodies.

Post-ore secondary faults identified by Kusov and others (1965b) are right- or left-lateral or normal-slip faults and thrust faults, such as the Western, Naurak, Kharh, Lagernoye, Awband, Sio-Sang, and Eastern Faults (fig. 7A–16; table 7A–2). These faults were followed by smaller scale faulting. The iron ore field was broken into step-like structures by these faults, and according to Kusov and others (1965b), horst and grabens were generated.

In general, Kusov and others (1965b) recognized that the Haji-Gak iron ore deposit is conformable with folded strata in the region and is confined to the limb of a monocline, which was folded again and fractured. The majority of orebodies are conformable with folded strata, but several of the orebodies cut folded strata. The main pre-ore folding was thought by Kusov and others (1965b) to be at the end of the Triassic and the beginning of the Jurassic during the Cymerian Orogeny. Post-ore folding probably occurred during Paleogene Alpine Orogeny. Both orogenic events would be post-ore with respect to a volcanogenic syngenesis of the iron orebodies.

There is tectonic activity taking place at the present time, which has resulted in the steep relief, intense erosion, steep slopes, and very high elevation. It is unlikely that weathering of the iron ores could have oxidized the ores in this environment.

7A.7 Alteration, Veining, and Mineralogy of the Haji-Gak Iron Ore Deposit

The mineralogy of the Haji-Gak iron ores varies throughout the deposit. The minerals in the iron deposit consist of ore and gangue minerals. The gangue minerals consist mainly of sulfide, carbonate, phosphate, and silicate minerals.

A number of hydrothermal alteration minerals are present within the Haji-Gak iron mineralized system. Hydrothermal alteration and metasomatism within the Haji-Gak iron deposit host rocks consist mainly of secondary sericite, which has microgranoblastic and local relict textures that develop into grey-colored zones that may be spotted, stratified, dense, or fragmental. Quartz and quartz-hematite veins contain sericite, hydromica, quartz, ore minerals, as well as chlorite, barite, apatite, sphene, and tourmaline. Carbonatization is marked by zones of grey, spotted, stratified, unsorted, granoblastic textured rocks comprising carbonate, quartz, ore minerals, sericite, and barite.

Table 7A–2. Features of faults of the Haji-Gak iron orebody.

[Kusov and others, 1965a,b. The faults are shown in figure 7A–16. M, meters; NA, not available]

Fault letter designation on map	Name of fault	Type of fault	Azimuth	Dip	Comments	Displacement
a	Western I	Left-lateral	220°–230°	85°	Western wall displaced to the southeast, slickensides	70 m.
b	Western II	Thrust fault	220°–230°	80°	Eastern wall displaced and thrust, fractured	Horizontal 20 m, vertical 15 m, displacement surface 25 m.
c	Western III	Thrust fault (irregular)	230°–270°	80°–85°	Western wall displaced and thrusted, slickensides	16 m.
d	Naurak I	Normal fault	250°–270°	75°–85°	Western wall dropped down and displaced, friction	Horizontal 10 m, vertical 7 m, surface displacement 13 m.
e	Naurak II	Normal fault	260°–270°	70°–80°	Eastern wall dropped down and displaced, brecciated ore	Horizontal 10 to 40 m, vertical 11 m, surface displacement 30 m.
f	Kharh	Thrust fault	270°–200°	75°–80°	Western wall displaced to the south, friction	Horizontal 120 m, vertical 50 to 55 m, surface 100 m.
g	Lagernoye	Left lateral	80°–90°	85°	Western wall displaced to the south, 8 m wide	20 m.
h	Awband	Right lateral	240°	85°–90°	Eastern wall displaced	35 m.
i	Central	Thrust fault	200°–240°	75°–85°	Western wall displaced, thrust under 45°	Surface 450 m, horizontal 730 m.
j	Sio-Jang	Thrust fault	5°–10°	80°	Northern wall displaced and thrust, slickensides, breccia	Surface 10 to 170 m.
k	Chapkul I	Normal fault	5°–10°	70°	Northern wall displaced, friction	95 m.
l	Chapkul II	Normal fault	50°	70°	Western wall displaced	Horizontal 350 m, vertical 70 m.
NA	Eastern	Thrust fault	40°–60°	80°	Eastern wall displaced	Horizontal 1,500 m, vertical 500 m.

Several different vein types are present in the Haji-Gak orebodies and in the surrounding host rocks. Post-magmatic veins and quartz veins are present in all rock types, but large veins are most common in sandy quartz-sericite slaty schist of the Kab Formation. The thickness of most veins is 1 to 1.5 m, but some are as much as 10 to 50 m thick with dips between 30° and 90°. Magnetite-hematite veins are common in the orebodies, in diabase bodies, and especially in volcanic flows and schist of the Awband and Green Schist Formations. These veins have thicknesses of between 0.5 and 1 m and locally up to 5 m. Carbonate veins are prolific in Haji-Gak Formation. The highest density of carbonate veins is along the fractured zones. Barite is also present in veins and lenses near the orebodies among rocks of the Awband Formation and most commonly along fractured and faulted zones. The barite-rich vein thickness is between 0.1 and 0.5 m and locally up to 1 m. Locally, barite veins lie in clusters a few meters wide and 100 m long.

Orebodies in the Awband Formation are divided into nonoxidized and semioxidized ores. Nonoxidized ores include pyrite-magnetite zones with high sulfur and magnesium concentrations (fig. 7A–18). The zones are massive (figs. 7A–13, 7A–14, and 7A–17), massive-banded, and spotted, containing mainly magnetite, hematite, pyrite, quartz, carbonate minerals, rarely chlorite, and sericite.

Semioxidized ores comprise mainly hydrogoethite-semimartite, hydrogoethite-hematite-semimartite, and carbonate-semimartite. Hydrogoethite-semimartite and hydrogoethite-hematite-semimartite ores are fine- and medium-grained, massive, massive-banded, porous, and form veins and lenses that comprise mainly hydrogoethite, goethite, magnetite, martite, hematite, quartz, carbonate minerals, and pyrite. Carbonate-semimartite ores are massive, massive-banded, and spotted, and form veins and lenses that comprise magnetite, hematite, pyrite, quartz, carbonates, rarely chlorite, and sericite.

Figure 7A–17. Photographs of outcrops of the Haji-Gak sedimentary iron deposit in Bamyan and Wardak Provinces from Peters and others (2007). (*a*) Photograph showing iron deposit at the crest of ridge and foliated schist in the foreground. (*b*) Photograph of joint U.S. Geological Survey-Afghanistan Geological Survey field reconnaissance team (2006)at exploration adit in iron ores of the Haji-Gak deposit. Photographs by Robert Bohannon, U.S. Geological Survey.

Figure 7A–18. Photographs of ores from the Haji-Gak iron ore deposit. (*a*) Photograph of hand specimen of mixed magnetite and semimartite iron ore. (*b*) Euhedral pyrite magnetite ore. Photographs from Afghanistan Geological Survey files (scale approximate). Photographs by the Afghanistan Ministry of Mines.

7A.8 Primary Nonoxidized Ores

The primary nonoxidized ores mainly are pyrite-magnetite ores. These pyrite-magnetite ores are present to a depth of 100 m, but are not well documented. The ores are dense, fractured, steel-black in color, and exhibit massive to banded and spotted textures with fine- to medium- and rare coarse-grained, xenomorphic (cathedral) and idiomorphic grains. The pyrite-magnetite ores mainly consist of iron

(56.24 to 68.80 wt. %, averaging 61.30 wt. % iron). Bands in the ores show massive-banded textures and contain impregnations of pyrite and non-ore minerals, as well as altered magnetite and hematite bands. Spotted ores are present near the contacts of the ore with the host rock and are characterized by sporadic and uneven disseminations of pyrite, siderite, and quartz, as well as sparse barite, calcite, and dolomite impregnations (Kusov and others, 1965a)

Ore minerals in the pyrite-magnetite ores are predominantly magnetite and pyrite, with rare hematite and martite. Magnetite is present as massive, xenomorphic masses with cataclastic textures. The content of magnetite in the pyrite-magnetite ore varies from 40 to 90 vol. % and the average content is 68 vol. % (figs. 7A–18 and 7A–19). Hematite is present as flakes between magnetite grains or in veins. The content of hematite in the pyrite-magnetite ores does not exceed 2 vol. %. Martite in the pyrite-magnetite ore is present as pseudomorphs (the edges of magnetite grains alter into martite), including pseudomorphed magnetite grains with pyrite inclusions. The content of martite does not exceed 5 vol. %. Siderite is an abundant mineral in pyrite-magnetite ores, especially along the ore-host rock contact. It is present as veins and veinlets that penetrate the magnetite masses. Siderite usually is adjacent to quartz and chlorite, and exhibits a fine-grained, granoblastic texture. The siderite content varies from 1 to 25 vol. % of the pyrite magnetite ore.

Gangue minerals in primary nonoxidized ores include carbonate minerals (calcite, dolomite and siderite), silicate minerals (quartz, chlorite), sulfide minerals (chalcopyrite, pyrrhotite, barite, and pyrite), and phosphate minerals. Calcite and dolomite vary from 5 to 6 vol. % and are present as spots in quartz veins with quartz, pyrite, and barite. Quartz is the most abundant non-ore mineral in the Haji-Gak iron deposits. It is present in three generations and comprises between 6 and 10 vol. % of the ores. The first generation of quartz formed almost simultaneously with magnetite. The second generation of quartz formed after magnetite and almost simultaneously with hematite. The third generation of quartz formed along with sulfide minerals and forms accumulations from 0.1 to between 10 and 30 centimeters (cm) thick. Early third generation quartz also contains pyrite inclusions. Late third generation quartz is adjacent to calcite, dolomite, and barite. Chlorite is present in banded textures with quartz, calcite, and barite. The chlorite content of most ores is 1 vol. %.

Pyrite crystals [0.01 to 5 millimeters (mm) in diameter] are unevenly disseminated throughout the primary nonoxidized iron orebodies (fig. 7A–19*a*) and also form dense impregnation bands; the content of pyrite averages 14 vol. % in the ores. Barite is sporadically dispersed throughout the pyrite-magnetite ore and makes up 2 vol. % of the ore. Barite is usually spatially adjacent to quartz and carbonate minerals and locally with pyrite; fills voids between quartz, pyrite, and magnetite grains; and forms veins and veinlets. Chalcopyrite (less than 0.2 mm in diameter) and pyrrhotite (up to 0.07 mm in diameter) also are rarely present with pyrite and siderite as inclusions, and these sulfide minerals combined constitute 1 vol. %.

The pyrite-magnetite ores require desulphurization and agglomeration and further metallurgical processing. Metallurgically harmful mineral mixtures in the ores are sulfur (sulfatic and sulfidic minerals, 4.75 wt. %),% phosphorus (0.05 wt. %), and zinc (less than 0.01 wt. %). The sulfidic sulfur occurs with barite, and its content is 0.04 wt. %. The sulfidic sulfur occurs with pyrite, and its content is 4.69 wt. %. Metallurgically nonharmful mineral mixtures in the ore are nickel 0.001 to 0.01 wt. %), copper 0.003 to 0.01 wt. %), cobalt trace amounts to 0.001 wt. %), silver (trace amounts), and manganese (trace amounts). Barium (0.001 to 0.06 wt. %) is present as barite.

7A.9 Primary Semioxidized Ores

Primary semioxidized orebodies contain hydrogoethite-semimartite, hydrogoethite-hematite-semimartite, and carbonate-semimartite ores. Tables 7A –3 and 7A –4 list the descriptions and mineral contents of primary semioxidized ores.

7A.9.1 Hydrogoethite-Semimartite Ores

Hydrogoethite-semimartite ores are predominant in the Haji-Gak iron deposit and extend from the surface to between 100 and 130 m deep. They are dense, steel-black in color with brownish tints, fine to medium-grained, xenomorphic, with massive-banding, and in places have spotted textures (fig. 7A–20*c*). The hydrogoethite-semimartite ores also display porous textures, which are most likely owing to leaching of nonmetallic minerals and to pyrite oxidation. The tops of the pores usually are covered with rims of hydroferric oxide minerals and carbonate minerals. The content of ore in hydrogoethite-semimartite orebodies is 52.29 to 68.32 vol. %, with an average content of 62.32 vol. %. Ore minerals of the hydrogoethite-semimartite ore include magnetite-martite, goethite, hydrogoethite, and magnetite.

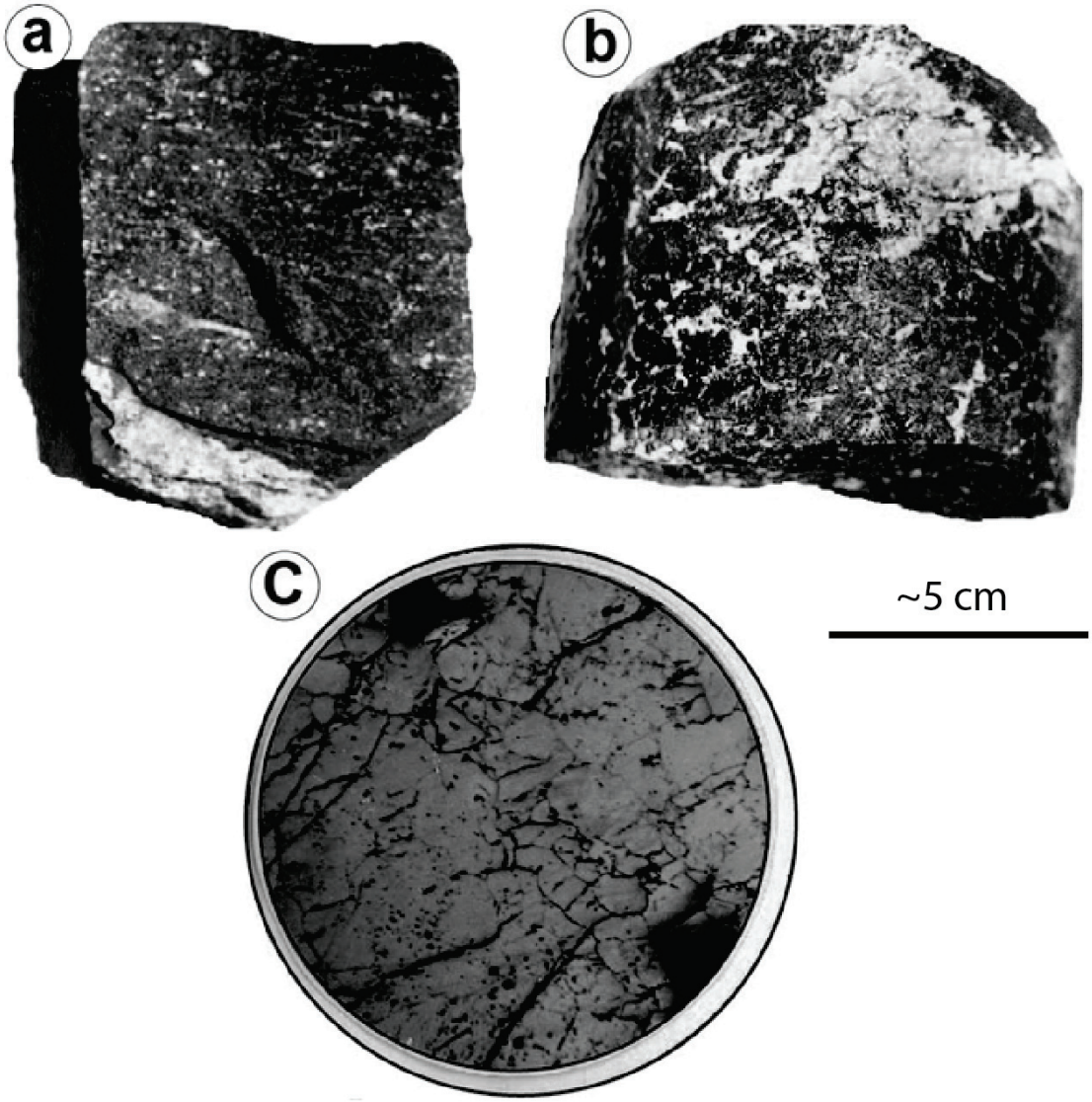

Figure 7A–19. Photographs of pyrite-magnetite ores of Haji-Gak iron deposit from Kusov and others (1965b). (*a*) Pyrite-magnetite ore with massive-banded texture, comprising ground mass, the thin bands formed by siderite and pyrite; from core hole 2 at a depth of 148 meters. The white spot at the bottom is quartzite. (*b*) Pyrite-magnetite ore with spotted texture. Magnetite is black, siderite is white, and pyrite is grey. Sample is from core hole 1 at a depth of 125.9 meters. (*c*) Magnetite that exhibits xenomorphic, coarse-grained texture and shows cataclasis; from thin section 150-I.

Table 7A–3. Description and mineral content of ore.

[Kusov and others, 1965a,b. All values are in percent. Ag, silver; Ba, barium content; $BaCo_3$, barium; Co, cobalt; Cu, copper; Ni, nickel; NA, not available; P_4, phosphorus ; V, vanadium; Zn, zinc; —, zero; <, less than]

Mineral	Primary nonoxidized, pyrite-magnetite ore		Primary semioxidized					
			Hydrogoethite semimartite ore		Hydrogoethite hematite semimartite ore		Carbonate semimartite ore	
	Range	Average	Range	Average	Range	Average	Range	Average
Ore minerals								
Magnetite	40–90	68	5–70	39	1–47	31	20–60	39
Pyrite	2–35	14	0–5	<5	0–6	—	0–10	2
Siderite	1–25	8	single grains	—	—	—	2–30	5
Hematite	0–2	<2	0–20	5	10–50	33	—	—
Martite	0–5	<5	1–80	20	2–55	19	1–18	10
Hydrogoethite	—	—	1–85	25	1–20	10	1–5	3
Chalcopyrite	single grains	—	—	—	—	—	—	—
Muscovite	—	—	single grains	—	—	—	—	—
Maghemite	—	—	single grains	—	—	—	—	—
Pyrrhotite	single grains	—	—	—	—	—	—	—
Non-ore minerals								
Quartz	1–10	6	1–25	7.5	1–8	4	0–8	3
Dolomite	1–6	2	0–2	1	0–2	—	15–50	28
Calcite	1–5	1	0–3	—	NA	NA	5–20	7
Chlorite	0–9	<1	0–5	—	0.5–8	—	—	—
Sericite	—	—	0–2	—	0–2	—	—	—
Ankerite	—	—	single grains	—	—	—	—	—
Actinolite	—	—	single grains	NA	0–1	—	—	—
Plagioclase	—	—	single grains	—	0–3	—	—	—
Gypsum	—	—	0–5	—	single grains	—	—	—
Magnesite	—	—	single grains	—	—	—	—	—
Talc	NA	NA	NA	NA	single grains	—	—	—
Barite	0–2	2	0–3	—	single grains	—	NA	NA
Harmful mixture								
Sulfatic (barite)	0.04	NA	0.04–1.97	0.11	NA	NA	0.06	NA
Sulfidic (pyrite)	4.69	NA	NA	NA	0.07	—	NA	NA
P_4	0.05	NA	0.02–0.09	—	0.046	—	0.05	NA
Zn	<0.01	NA	< 0.01	NA	NA	—	0.01	NA
Good mixture								
Ni	0.001–0.01	NA	0.03–0.02	NA	0.001	—	trace-0.003	NA
V	—	NA	NA	NA	0.001	—	trace-0.003	NA
Cu	0.003–0.01	NA	trace-0.01	NA	0.001	—	traces	NA
Co	trace-0.001	NA	0.002–0.005	NA	0.001	—	trace-0.01	NA
Ag	traces	NA	NA	NA	—	—	—	—
Mn	traces	NA	NA	NA	—	—	—	—

Mineral	Primary nonoxidized, pyrite-magnetite ore		Primary semioxidized					
			Hydrogoethite semimartite ore		Hydrogoethite hematite semimartite ore		Carbonate semimartite ore	
	Range	Average	Range	Average	Range	Average	Range	Average
$BaCo_3$ (Ba)	0.001–0.06	NA	NA	NA	0.01–0.06	0.02	—	—

Table 7A–4. Description and mineral content of ore, showing grain size.

[Kusov and others, 1965a,b. Values are in millimeters. NA, not available; —, zero]

Mineral	Primary nonoxidized, pyrite-magnetite ore		Primary semioxidized					
			Hydrogoethite semimartite ore		Hydrogoethite hematite semimartite ore		Carbonate semimartite ore	
	Range	Average	Range	Average	Range	Average	Range	Average
Ore minerals								
Magnetite	0.01–1	0.2	0.01–4	0.2	0.01–3	0.3	0.02–4	0.3
Pyrite	0.1–5	0.3	as large as 4	—	0.01–0.4	0.2	0.1–4.5	0.3
Siderite	0.1–4	0.2	as large as 4	—	—	—	0.2–4	0.5
Hematite	as large as 3	—	as large as 5	—	0.1–6	0.5	—	—
Martite	as large as 0.2	—	0.01–1	0.2	0.01–0.2	0.1	0.01–3	0.1
Hydrogoethite	—	—	0.01–0.5	0.4	0.01–0.5	0.2	0.1–0.3	0.2
Chalcopyrite	as large as 0.2	—	—	—	—	—	—	—
Muscovite	—	—	as large as 1	—	—	—	—	—
Maghemite	—	—	as large as 1	—	—	—	—	—
Pyrrhotite	as large as 0.07	—	—	—	—	—	—	—
Non-ore minerals								
Quartz	0.01–1	0.3	as large as 5	0.15	0.01–0.1	0.05	0.01–0.5	0.1
Dolomite	0.2–5	0.5	0.2–5	2	0.2–5	0.4	0.02–6	0.3
Calcite	as large as 5	0.3	0.1–6	0.3	NA	NA	0.05–4	0.3
Chlorite	as large as 5	—	as large as 1	—	0.5–2	0.4	—	—
Sericite	—	—	as large as 1	—	as large as 0.2	—	—	—
Ankerite	—	—	as large as 2	—	—	—	—	—
Actinolite	—	—	as large as 3	NA	0.1–2	0.5	—	—
Plagioclase	—	—	as large as 5	—	0.3–9	0.1	—	—
Gypsum	—	—	0.2–6	0.5	as large as 5	—	—	—
Magnesite	—	—	as large as 2	—	—	—	—	—
Talc	NA	NA	—	—	as large as 0.2	—	—	—
Barite	as large as 0.5	—	0.1–0.3	0.5	as large as 0.2	—	NA	NA

Hydrogoethite-semimartite ore formed as a result of supergene processes on pyrite-magnetite ores (Kusov and others, 1965b). Magnetite is the predominant mineral in hydrogoethite-semimartite orebodies, and its content varies from 1 to 70 vol. %, with an average of 39 vol. %. The characteristic grain size and structures are similar to the magnetite in pyrite-magnetite ores. Magnetite grains display three main types of texture. The first is xenoblastic where magnetite grew during metamorphism without developing crystal faces (fig. 7A–20*c*). The second texture is hypidioblastic, where newly formed subhedral crystals are bounded in part by characteristic crystal faces (figs. 7A–18 and 7A–20*a*). The third texture is recrystallization near the fault zones (fig. 7A–20*b*). Martite is a hematite pseudomorph of magnetite that constitutes 1 to 80 vol. % of the orebody and is unevenly disseminated throughout the ore. The martite has the following forms:

- rims that develop along pseudomorph cleavage planes and fractures within magnetite grains; during intensive replacement, the rims form a web or acquire a spongy texture
- replacing magnetite along cracks or forming rims along the magnetite edges, creating a mesh texture
- forming small spotted grains with zoned rims
- pseudomorphing magnetite either along cracks or entire magnetite grains

Iron hydroxide minerals (mainly hydrogoethite) are well developed and dispersed in the oxidation zone. The content of iron hydroxides in ore is 85 vol. %,with an average content of 25 vol. %. Iron hydroxide minerals formed from oxidation of magnetite, pyrite, siderite, and partially martite (the process of magnetite replacement by iron hydroxides is more intensive than martitization). Hydroxides replace magnetite in different ways, such as accumulations or webs (fig. 7A–21*b*). Hematite is dispersed unevenly and comprises 20 vol. % of ore, with an average of 5 vol. %. Hematite in massive ores fills voids between magnetite grains and also forms veins and veinlets. In banded ores, hematite forms 0.5-mm-thick sheets. Hematite formed in two generations. The first was subsequent to magnetite and formed banded accumulations and inclusions among magnetite grains. The second is characterized by monomineralic veins with quartz. Siderite developed near the orebody contact with dolomitic marble and schist. Siderite has been oxidized into iron oxide minerals that occur in single grains or in accumulations between magnetite grains.

Gangue minerals in the hydrogoethite-semimartite ores include silicate (mica, quartz, talc, plagioclase, zircon, and actinolite), sulfide (pyrite), and carbonate (siderite, carbonate) minerals. Quartz is the predominant non-ore mineral and occurs in three generations within hydrogoethite-semimartite ore, as in the pyrite-magnetite ores in spotted forms or veins. Muscovite forms sheets in the groundmass of orebody I with isometric magnetite grains and was developed during the formation of hematite and the sulfidic mineralized zones. Talc and gypsum also are secondary minerals in hydrogoethite-semimartite ores. Plagioclase and actinolite are remnant minerals in the ores. Zircon is a very sparse mineral in the orebodies. Pyrite in primary semioxidized ores is present as impregnations and relicts that are unevenly dispersed within the host rocks. The content of pyrite in the iron ores does not exceed 5 vol. %, and the mineral is absent in ores that are at a depth greater than 50 to 80 m. Carbonate minerals are also remnants within the ore.

Metallurgically harmful elemental mixtures in the hydrogoethite-semimartite ores include sulfur, phosphorus, and zinc (Kusov and others, 1965b). Sulfur is highly abundant with concentrations from 0.04 to 1.97 wt. %, with an average of 0.11 wt. %, and is present as sulfatic (barite and gypsum) and sulfidic (pyrite) sulfur. The content of sulfur in sulfatic sulfur does not exceed 0.04 wt. %. Phosphorus appears in isomorphous mixtures, with a concentration that varies from 0.02 to 0.09 wt. %. Zinc concentration in ores usually does not exceed 0.01 wt.%. Metallurgically useful elemental mixtures are manganese, nickel (0.03 to 0.02 wt. %), cobalt (0.002 to 0.005 wt. %), copper (trace to 0.01 vol. %), silver, and barium.

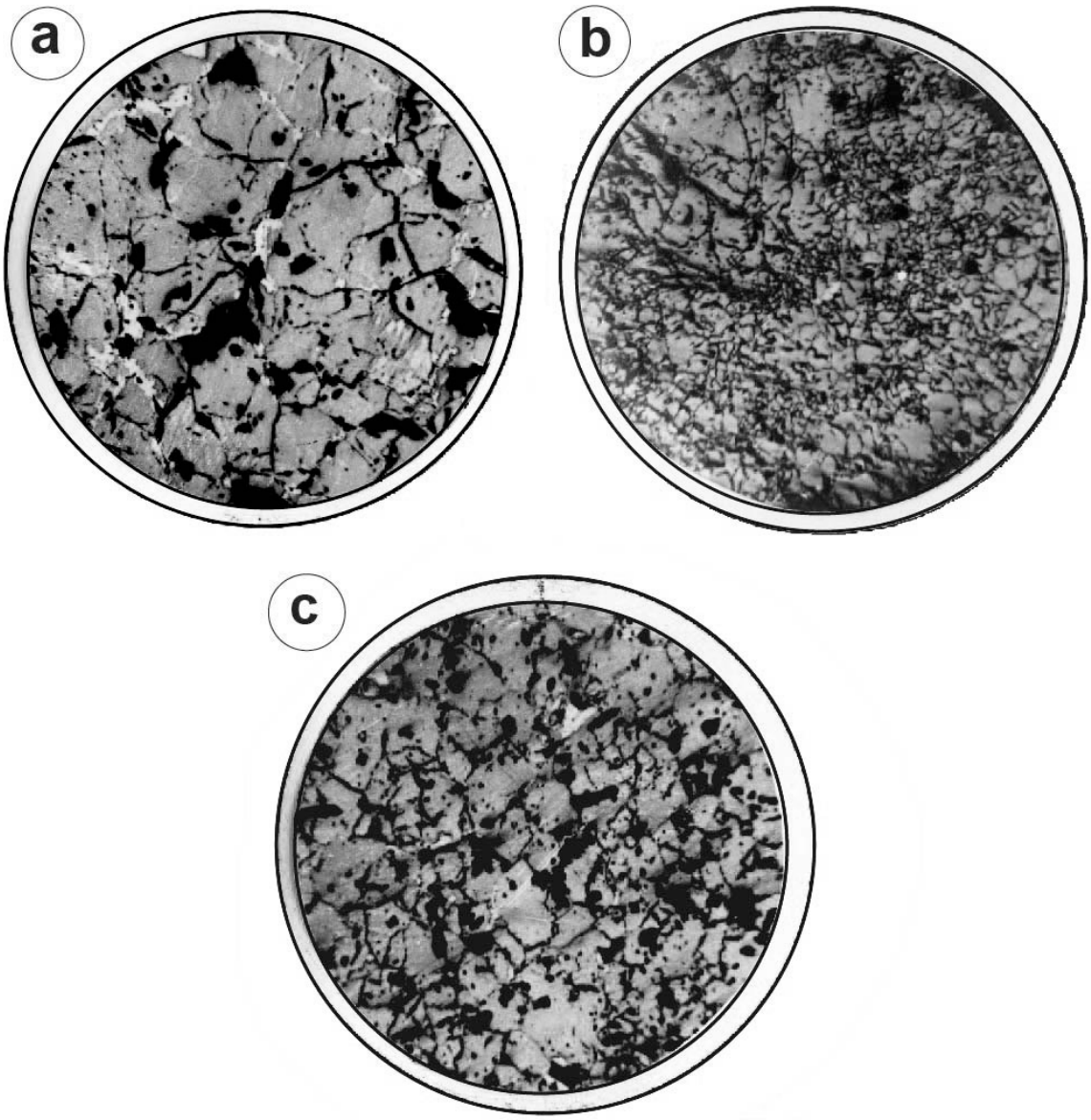

Figure 7A–20. Photographs of hydrogoethite-semimartite ore from Kusov and others (1965b); scale not recorded. (*a*) Hydrogoethite-semimartite ore with massive hypidioblastic texture. Magnetite (dark grey) underwent martitization (light-grey) and developed pores (black); from thin section 1638-I. (*b*) Hydrogoethite-semimartite ore that has been recrystallized. Magnetite (grey) includes quartz (dark grey); from thin section 454-I. (*c*) Hydrogoethite-semimartite ore with massive texture. Pores (black) are superjacent; magnetite (light-grey) grains illustrate xenoblastic texture; from thin section 454-I.

7A.9.2 Hydrogoethite-Hematite-Semimartite Ores

Hydrogoethite-hematite-semimartite ores are not abundant in the Haji-Gak iron deposit. They are fine- to medium-grained banded ores that are dense and steel-black in color (fig. 7A–22). Vugs are dispersed unevenly and range in size from 0.1 to 5 mm in diameter. The iron content varies from 59.49 to 65.68 wt. %,with an average of 62.66 wt. %. The hydrogoethite-hematite-semimartite ores are present as lenses (25.5 m thick from surface and 340 to 650 m long along the strike). Hydrogoethite-hematite-semimartite ores are similar to hydrogoethite-semimartite ores, and during the estimation of ore reserves, both ores were considered to be a single commercial ore type (table 7A–1). The only difference between the two ores is a higher concentration of hematite and banded textures in the hydrogoethite-hematite-semimartite ore (fig. 7A–22). These ores are present in oxidized zones at depths between 100 and 130 m from the surface.

Ore minerals in the hydrogoethite-hematite-semimartite ores include magnetite, hematite, martite, and hydrogoethite (Kusov and others, 1965b). Magnetite (with a grain size from 0.01 to 3 mm in diameter) content is 1 to 47 vol. %; hematite (with a grain size from 0.1 to 6 mm in diameter) content is 10 to 50 vol. %; martite (with a grain size from 0.01 to 0.1 mm in diameter) content is 2 to 55 vol. %; and hydrogoethite (with a grain size from 0.01 to 0.2 mm in diameter), content is 1 to 20 vol. %.

Gangue minerals include silicate (quartz, chlorite, plagioclase, actinolite, talc, and sericite), carbonate (carbonate and dolomite), and sulfide and sulfate (barite, gypsum, and pyrite) minerals. Metallurgically harmful elemental mixtures in the hydrogoethite-hematite-semimartite ores are sulfur and phosphorus. The sulfur content is 0.07 wt. %, and the phosphorous content is 0.046 wt. %. Metallurgically useful elemental mixtures in the hydrogoethite-hematite-semimartite ores are nickel, vanadium, copper, and cobalt. The content of each element does not exceed 0.001 wt. %. Barium was identified at 0.01 to 0.06 wt. %, with an average of 0.02 wt. %.

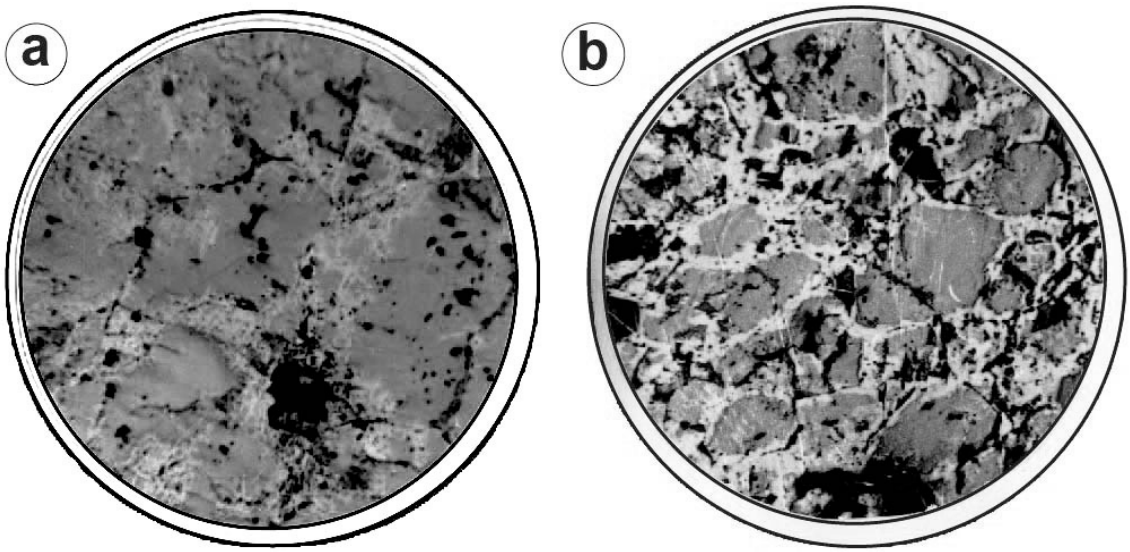

Figure 7A–21. Photographs of martite-bearing ores from Kusov and others (1965b); scale not recorded. (*a*) Martite (light grey)replaces magnetite (dark grey), creating a web or spongy texture. Dark-grey loops are iron oxide minerals, and areas in black are the pores and quartz. From thin section 1733. (*b*) Photograph of martite (white) replacing magnetite (grey), creating a mesh texture. Black is pores, and dark grey is the iron oxide minerals. From thin section 3g.

7A.9.3 Carbonate-Semimartite Ore

Carbonate-semimartite ore is less abundant than the other ores and occurs along the transitional zone between hydrogoethite-semimartite and iron ores in dolomitic marble and dolomitic limestone. Carbonate-semimartite ore is dense, mainly spotted (fig. 7A–23*a*), with a banded texture (fig. 7A–23*b*), and fine- to coarse-grained. The bands of the ore comprise magnetite and dolomite.

Ore minerals in the carbonate-semimartite ores include magnetite, martite, siderite, and hydrogoethite. Gangue minerals include silicate, such as sparse quartz; carbonates, such as dolomite and calcite; and sulfides, such as pyrite (Kusov and others, 1965b). Metallurgically harmful elemental mixtures include sulfur, phosphorus, and zinc. The content of these components is very low; sulfur content is 0.06 wt. %, phosphorus content is 0.05 wt. %, and zinc content is 0.01 wt. %. Metallurgically useful elemental mixtures in the carbonate-semimartite ores include nickel (trace amounts to 0.003 wt. %), vanadium (trace amounts to 0.003 wt. %), copper (trace amounts), and cobalt (trace amounts to 0.01 wt. %). A carbon dioxide content of 13.35 wt. % was also determined.

7A.9.4 Fragmental Ore

Fragmental ores are represented by a single industrial type of ore, hydrogoethite-semimartite ore. Fragmental ores are present as talus in loamy sand and as ore fragments and rubbles of quartz, schist, and dolomitic marble. The ore fragments are present as boulders, colluvial rubble, and in places as subrounded cobbles of hydrogoethite-semimartite, hydrogoethite-hematite-semimartite, and carbonate-semimartite ores. Fragmental ores are rich in iron. Metallurgically harmful elemental mixtures in the fragmental ores include sulfur and phosphorus. The content of these components is very low and it does not impact the ore quality. Metallurgically useful elemental mixtures include nickel, vanadium, copper, and cobalt. The total content of useful elemental mixtures is approximately 0.01 wt. %.

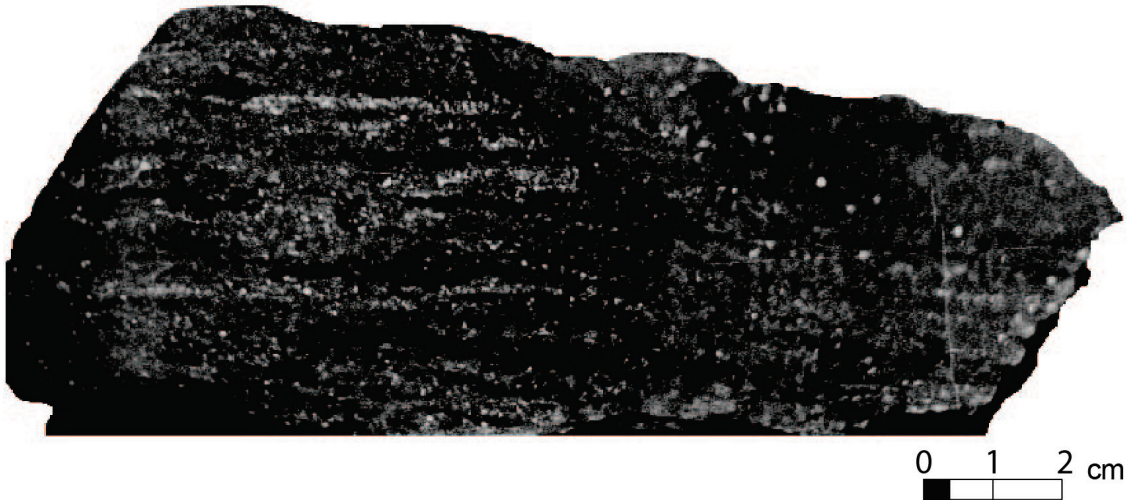

Figure 7A–22. Photograph of hydrogoethite-hematite-semimartite ore with banded texture from Kusov and others (1965b). The light grey bands are hematite, and the dark grey bands are martitized magnetite from sample 6, adit 1.

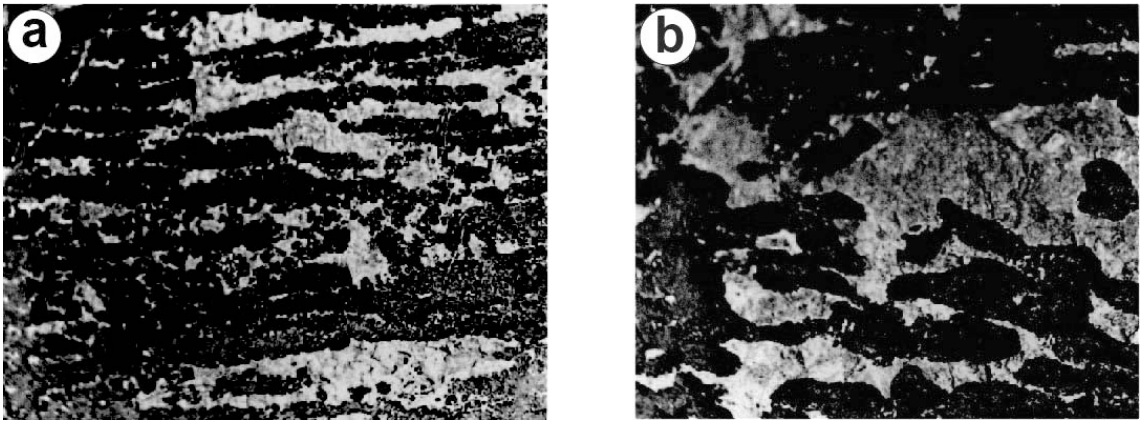

Figure 7A–23. Photographs of carbonate-semimartite ore with banded texture from Kusov and others (1965b); scale not recorded. (a) Photograph of carbonate-semimartite ore with banded texture, showing dolomite (white) and altered magnetite (black); sample K-12-1. (b) Carbonate-semimartite ore with spotted texture; marble (white) and martitized magnetite (black); sample K-12-2.

7A.10 Genesis of the Haji-Gak Iron Ores

A genetic model of the Haji-Gak iron deposit was proposed by Kusov and others (1965b). It is an epigenetic model derived from observations made on the geologic host rock and the inferred environment of deposition. The iron ore deposits of the Haji-Gak iron deposit are hosted by the Neoproterozoic(?) Awband Formation, which comprises sericite and quartz-sericite schist, quartz-sericite schist (derived from acidic tuff), carbonate-chlorite-sericite schist (derived from tuff),

marble, and dolostone. The Awband Formation rocks have been folded, faulted, and intruded by diabase. The ore in the Haji-Gak iron deposit area is controlled by stratigraphy and structure.

Structural and stratigraphic control of the Haji-Gak iron deposit and other peripheral areas of the iron ore were thought by Kusov and others (1965b) to be owing to the proximity of the Haji-Gak-Kharzar regional deep fault zone. Therefore, the ores were thought to be spatially and genetically related to small plagiogranite, granodiorite, and quartz diorite intrusive bodies, which also are located along the same fault zone as the iron deposits. The ores and the intrusive bodies were proposed as products from the same magma source but formed at different times. The regional fault and fault splays were hypothesized to be the channels for the intrusive bodies (silicate melts) and for the migration of the iron ore solutions. The orebody shape was caused by alteration of favorable rocks (schist derived from tuff, dolomitic limestone, and marls) or by ore precipitation in the open cracks. These suppositions are compatible with processes that take place during volcanogenic ore genesis also.

The contact between the iron orebodies and host rocks locally produced remnants of host rocks contained within the orebodies. The sharp and straight contact between host rocks (sandy quartz-sericite schist and sericite quartzite) and iron orebodies were thought by Kusov and others (1965b) to be formed by differences in permeability of the host rocks. The sharp and straight cross-cutting orebodies (IX, XIII; fig. 7A–24*b*) indicated the formation of orebodies in open spaces. Gradational, irregular, and wavy contacts of orebodies (I, IX; fig. 7A–24) with marl, dolomitic limestone, and schist (derived from tuff) indicate metasomatic replacement of the host rocks by the iron ore. Iron orebodies contain remnants of host rocks, such as schist with thin iron ore veins, which have been altered into sericitic quartzite during hydrothermal processes. The schistose texture of these remnants coincides with banded ore and retains the same spatial orientation as the host rocks (figs. 7A–15 and 7A–24). These observations also are compatible with processes that are coeval with volcanism.

Change in the footwall of ore host rocks was thought by Kusov and others (1965b) to be owing to alteration near the orebodies from the introduction of quartz and sericite and replacement of the host rocks rather than by syngenetic processes. Propylitization and carbonation were also thought to have taken place distal from the orebodies forming metasomatic carbonatite.

Mineralogical, geochemical, petrographical, textural, and structural genetic criteria of the iron ores were thought by Kusov and others (1965b) to be marked locally by massive, banded, and spotted textures, but mainly by fine- and medium-grained textures, as well as by sandy and occasionally hypidiomorphic textures. Banded textures in the ores mainly are present parallel to the schistosity and represent replaced schistose host rocks, whereas replacement massive textures are likely to be present in carbonate rocks. These textures also are compatible with volcanogenic and syngenetic processes. Relict minerals and textures interpreted to be from incomplete replacement by Kusov and others (1965b) may also be owing to syngenetic processes. The remnants (relicts) of actinolite, sericite, and chlorite were preserved in banded ores, which occur during alteration of schists, and carbonate relicts and local pseudomorphs of magnetite along the rhombs of dolomitization were preserved in massive ores.

The paragenetic sequence of minerals in primary nonoxidized ore is magnetite, muscovite, hematite, quartz, pyrite, siderite, albite-oligioclase, barite, actinolite, and chlorite. The presence of associated element mixtures in ore, such as nickel, copper, barium, vanadium, zinc, and sometimes cobalt, silver, and molybdenum, in combinations with primary iron, silica, potassium, carbon dioxide, and sulfur, also indicates hydrothermal ore-bearing solutions were involved in ore genesis. The weakly expressed, vertical primary zonation of orebodies, caused by high concentrations of ore sulfide minerals (mainly pyrite) and copper (as chalcopyrite) at a depth of 100 to 130 m and the low concentration of hematite, was thought by Kusov and others (1965b) to indicate hydrothermal endogenic ore formation; however, the same zonation of orebodies can also be accounted for by folding or metasomatic reworking of stratabound, syngenetic orebodies.

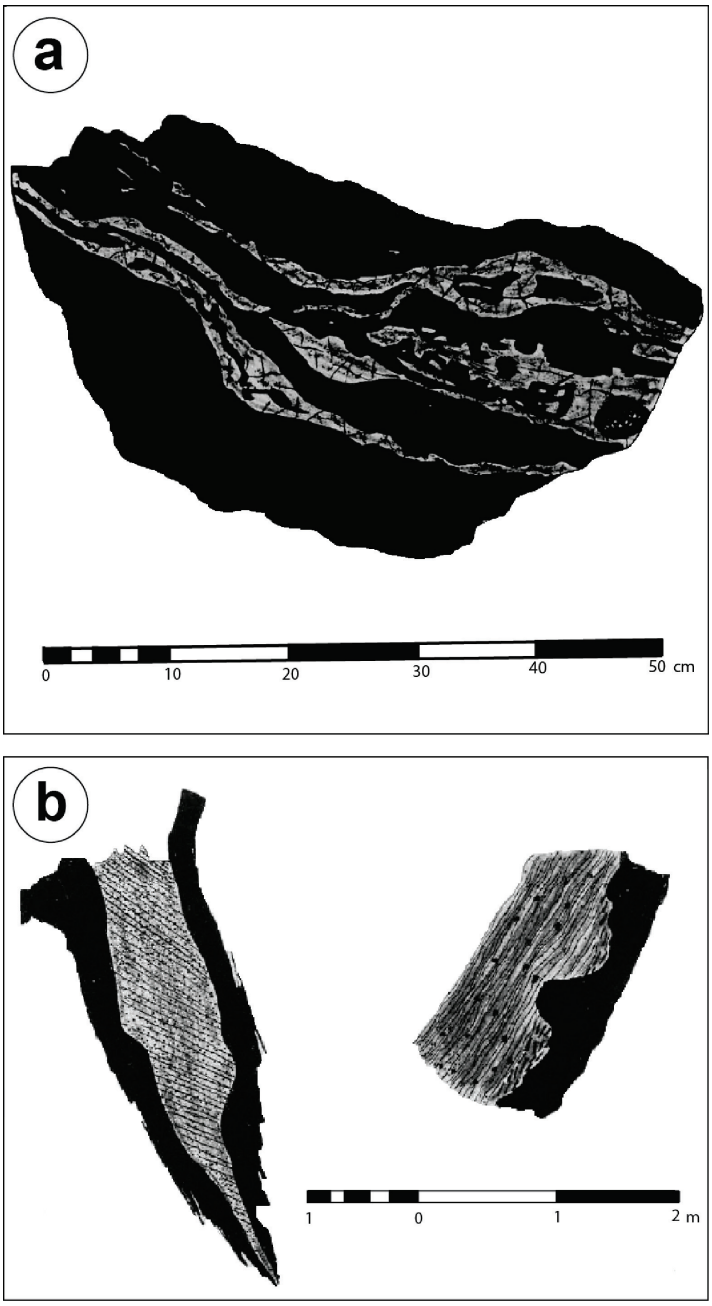

Figure 7A–24. Photographs of Haji-Gak iron ores showing layering from Kusov and others (1965b). (*a*) Remnants of sericite quartz in ore; from shaft # 1 at an interval of 180 to 189 meters. (*b*) Remnants of sericite quartz (light) among hydrogoethite-semimartite ore (black); the contact of hydrogoethite-semimartite ores with carbonate-chlorite-sericite schist is shown.

The source of ore-bearing epigenetic solutions was postulated by Kusov and others (1965b) to be a deep magmatic center. The product of this hypothetical magmatic center was also thought to have undergone magmatic distillation with separation into silicate melt and a gas phase. The intrusive bodies were speculated to be the small intrusions of plagiogranite, granodiorite, quartz diorite and hydrothermal-metasomatic mineralization (ore veins, barite veins, metasomatic carbonatite, and alteration of footwall rocks). These intrusive bodies, along with co-magmatic volcanic rocks found at Haji-Gak are also typical of volcanogenic environments. The hydrothermal ore-bearing solutions were formed from gas phases. Kusov and others (1965b) thought that the primary components of geochemical hydrothermal solutions, based on the footwall alterations, are Fe, Si, Ca, K, carbon dioxide, sulfuric

acid, Ba, and Mg, followed by Na, Zn, Ni, Cu, V, Co, Ag, and Mo, indicating a process by which the formation of hydrothermal solutions evolved as a gas that migrated into the host rocks, followed by the alteration of the host rocks and cooling that led to transition into the liquid phase.

The main ore host structures were interpreted by Kusov and others (1965b) to be the Haji-Gak-Kharzar fault that splayed from the main faults followed by folding and intensive fracturing. Rather than postdating syngenetic ore, these structural zones were thought to serve as ore-bearing solution pathways from a magmatic center to sites of ore precipitation. Furthermore, the contact between the heterogeneous Awband Formation and the relatively homogeneous Kab Formation was faulted prior to ore formation and the footwall of the ore zone lies along this contact. Therefore, the Kab Formation rocks are interpreted by Kusov and others (1965b) to have served as an impermeable barrier during ore formation.

Beds and lenses of marl, dolomitic limestone, and carbonate-chlorite-sericite schist (derived from tuff) are interpreted by Kusov and others (1965b) to be thoroughly replaced by iron ores, such that small beds are located between impermeable rocks or partially permeable rocks and thick beds and were not limited in permeability (orebodies I, and IX, fig. 7A–25*b*). Further interpretation of the epigenesis of the orebodies by Kusov and others (1965b) is as follows:

> "Orebodies VII and XIII coincide with longitudinal folded structures or cross-cutting faults, which were formed before ore formed. Faulted and folded structures, in the areas of unfavorable for replacement of rocks, such as sericite quartzite, quartz-sericite schist, alkaline volcanic rocks, plagiogranite, granodiorite, and quartz diorite, coincide with small quartz-hematite veinlets and veins. The veinlets and veins in dolomitic limestone marl and carbonate-chlorite-sericite schist served as a path for migration and interoperability of ore-bearing solutions with indicated rocks. Fractures formed before ore deposition allowed the circulation of ore-bearing solutions and formed favorable conditions for permeability within the host rock that underwent replacement."

Epigenetic interpretations of ore formation by Kusov and others (1965b) are that hypogene ore genesis took place in three stages. The first stage is marked by dolomitization, silicification of the host rocks, and precipitation of magnetite, hematite (iron mica), and quartz and involves deposition of magnetite with quartz and deposition of magnetite-hematite. The second stage of mineralization is characterized by carbonatization, sericitization of the host rocks, and the deposition of hematite, pyrite with quartz, siderite, and barite. During this phase, barite inclusions formed in the iron ores and veinlets of hematite with quartz grew in massive sulfide-rich (mainly pyrite) areas. The first two stages constitute the main ore-forming stages. The third phase involves the formation of veins, veinlets, siderite inclusions, and occasionally pyrite with quartz and barite with carbonate minerals and quartz. During the third phase, the ore-bearing solutions were not enriched in iron, and as a result, during interaction with the host rocks, such as limestone and dolomite, siderite was formed. The high content of sulfide minerals (mainly pyrite) indicates a nonoxidized environment. The deposit was thought to have formed at moderate depths under moderate temperatures as indicated by the ore mineralogy, the spatial connection of ore with the intrusive bodies, and the ore structures.

A final supergene overprinting stage of ore formation converted the nonoxidized pyrite-magnetite ore with hematite and siderite into semimartite and in places into martite ores containing iron hydroxide minerals. The alteration of the mineral content was considered by Kusov and others (1965b) to be mainly by oxidation of ore minerals and also by partial decomposition of non-ore minerals. Maghemite, martite, goethite, and hydrogoethite were derived from primary ore minerals. Magnetite was partially replaced by supergene hematite (martite). Locally, martite was oxidized to goethite and hydrogoethite. Frequently, magnetite was oxidized to iron hydroxides, and locally magnetite was altered to maghemite. Primary hematite was altered. Pyrite was thoroughly oxidized, and left behind iron ochre in pores after the leaching process. Carbonate minerals, quartz, and magnesium were leached and siderite was oxidized to residual iron hydroxide minerals.

Quartz, chlorite, sericite, and some other minerals in the supergene ores are typical residual products. The main change of physical properties in the supergene ores is the development of porous

textures. As a result of pyrite oxidation and of partial leaching of the non-ore minerals the ores became enriched in iron.

Although mesoscopic textures indicate hydrothermal-metasomatic conditions during the formation of the Haji-Gak iron deposit, the genesis of the deposit is not well understood. The main reason is that the primary ore's relations among host rocks at depth have not been well studied.

The age of the Haji-Gak iron deposit, based on tectonic, magmatic, and stratigraphic conditions known in the area, was thought to be Early Jurassic by Kusov and others (1965b), who based this interpretation on the spatial association of the ores with tectonic and magmatic processes that are thought to be Early Jurassic. The volcanic rocks, plagiogranite, granodiorite, and quartz diorite contain cross-cutting veins and veinlets, as well as hematite inclusions, magnetite, or hematite-magnetite-quartz. Orebodies VI and XI (fig.7A–25*b*) cut granodiorite and plagiogranorite dikes. Taking into consideration the connection of ore and intrusions with one magmatic center, the time of their formation is synchronized. Metamorphism of the ore was thought by Kusov and others (1965b) to be absent, whereas some host rocks such as the Devonian and Cretaceous ages were not considered metamorphosed. The connection of ore formation with fractured structures of post-Devonian age indicated to Kusov and others (1965b) that the Haji-Gak iron deposit was of Early Jurassic age.

7A.11 Ore Reserve Estimation and Reserves and Resources

In 1963 and 1964, the Afghanistan Geological Survey Russian contractor measured and estimated the iron resource of the Haji-Gak iron deposit. The western part of the Haji-Gak area was intensively explored, while the central and eastern parts were explored less.

This exploration work included making maps at a scale of 1:50,000 and 1:10,000, drilling holes, and digging trenches, adits, and shafts. Samples were collected, and prospect lines (traverses) were drawn. The data collected from trenches, shafts, and prospect lines were used to create vertical cross sections and horizontal plans, which were then used to calculate the end areas of the geometrical figures and then used to calculate the volume of the ore.

Primary ores are subdivided into 16 orebodies that have been designated by Kusov and others (1965a,b) by roman numerals I through XVI (fig. 7A–25). Fragmental ores are subdivided into four orebodies (A, B, C, and D; fig. 7A–25). The natural ores were further subdivided into resource categories A, B, C_1, and C_2, and separate plans were drawn for the orebody that was explored. The calculated tonnages for the reserves and resources are listed in tablet 7A–5.

7A.11.1 Prospects and Anomalies

A number of non-iron deposits, prospects, and occurrences are present in the Haji-Gak iron deposit and adjacent subareas. Known prospects and anomalies are the Haji-Gak barite, Haji-Gak limestone, and Haji-Gak sandstone deposits.

Table 7A–5. Tabulation of reserves and resources of the Haji-Gak iron deposit.
[Tabulation of data from Soviet exploration in the 1960s. NA, not available; wt. %, weight percent]

Soviet category	Equivalent classification	Ore type	Ore, in million metric tons	Iron, in wt. %	Sulfur, in wt. %
A	Measured or proven	Oxidized ore	9.1	62.52	0.14
B	Measured or proven	Oxidized ore	19.2	62.69	0.09
C_1	Indicated or probable	Oxidized ore	65.1	62.15	0.13
C_1	Indicated or probable	Primary ore	16.2	61.3	4.56
C_1	Indicated or probable	Fragmental ore	1.2	60.62	0.08
C_2	Inferred or possible	All ore types	3,143	NA	NA
C_2	Inferred or possible	Fragmental ore	2.9	NA	NA
P_2	Hypothetical resources	All ore types	1,333.3	NA	NA
P_2	Hypothetical resources	Fragmental ore	8.6	NA	NA
		Total	1,769.9		

7A.11.1.1 Haji-Gak Barite Deposit

The Haji-Gak iron AOI contains five locations of barite mineralization. Barite ore occurs as veins 0.2 to 1.2 m thick and 15 or 25 to 135 m long in Proterozoic chlorite-sericite schist. In addition, barite debris has been found over an area of 10 km^2. The speculative reserves of the largest vein are 36,200 metric tons (t) with an average barium oxide content of 56 percent.

7A.11.1.2 Haji-Gak Limestone Deposit

The 64-m-thick Upper Devonian limestone extends for at least 800 to 900 m, for an area of 45 km^2, to a depth of 60 m, and contains 49.08 to 54.7 percent calcium oxide. The limestone can be used as flux raw material. The speculative reserves are 3.5 Mt.

7A.11.1.3 Haji-Gak Sandstone Deposit

The deposit comprises Upper Devonian quartz sandstone that is 50 m thick and contains 93.66 to 97.31percent percent silicon oxide. The speculative reserves are 650,000 t. A deposit of refractory rock represented by a lenticular body of quartzite-like sandstone and quartzite, 32 to 70 m thick, resting in Upper Devonian carbonate sequence, is located in the area of the Haji-Gak iron deposit. The quality of the raw material is suitable for manufacturing class-II dinas.

7A.12 Northeastern and Farenjal Haji-Gak Subareas

Several prospects and anomalies are present in the Northeastern Haji-Gak and Farenjal subareas of the Haji-Gak iron AOI (figs. 7A–26 and 7A–27). To the northeast of the main Haji-Gak mine (Haji-Gak prospect) subarea, several additional mineral occurrences similar to Haji-Gak are present, such as Khaish, Zerak, Kharzar, Chui, Sausang, Kharkiz, Darre-i-Neelee, and Surkh-i-Parso (fig. 7A–27). The Northeastern Haji-Gak subarea contains the Kharzar, Khaish, Chuy, and Zerak sedimentary-rock hosted iron deposits that have been explored. The largest of these iron prospects adjacent to the Haji-Gak prospect subarea is the Khaish prospect in Bamyan Province, which is hosted in the same Proterozoic rocks as Haji-Gak. The Zerak iron occurrence in Baghlan Province lies within a fault zone, and three 90- to 450-m-long and 12- to 75-m-wide hematite magnetite zones have been discovered to date. Speculative resources are 20 Mt iron ore grading up to 62.5 wt. % iron. The Khaish, Zerak, Kharzar, Chui, and Sausang iron prospects are considered eastward continuations of the Haji-Gak deposit. The ore content, the deposition processes, the shape, and the host rocks of the ores in these prospects are similar to Haji-Gak. The total prospecting reserves in these extensions is 300 Mt (Kusov and others, 1965).

Table 7A–6. Location reserves and ore types of eastern prospects in the Northeastern Haji-Gak subarea.
[British Geologic Survey, NA, not available; wt. %, weight percent]

Name	Longitude	Latitude	Reserves, in million metric tons	Ore type	Iron, in wt. %
Khaish	34°43′55″N	68°12′30″E	117	hematite and magnetite	55.54
Kharzar	34°41′46″N	68°09′12″E	~10 [1]	hematite, magnetite, and martite	62.76
Chuy	34°45′37″N	68°13′00″E	NA	hematite and magnetite	56.93
Zerak	34°46′36″N	68°15′12″E	20	hematite and magnetite	56.93
Sausang	34°45′08″N	68°15′45″E	300	hematite and magnetite	NA

[1]Assuming more than 100 meters along the strike

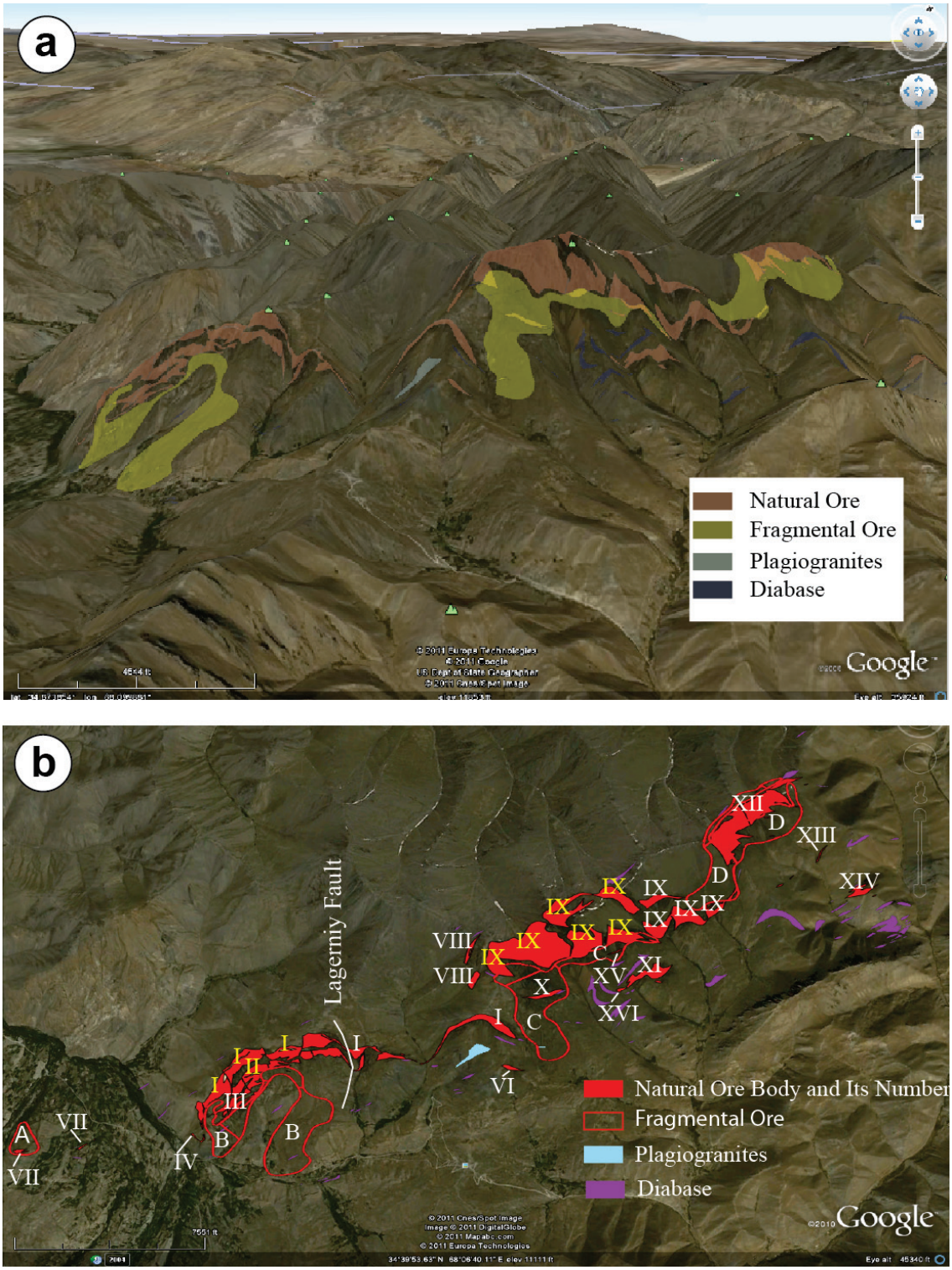

Figure 7A–25. Google Earth image with superimposed Haji-Gak iron orebodies. (*a*) Tilted image showing different types of orebodies. (*b*) Areal view showing orebodies and their designations.

These occurrences are described by Brueckl (1935, 1936), Momji and Chaikin (1960), and Bybochkin and Kurotchenko (1961). The iron occurrences are considered to be eastern extensions of the Haji-Gak iron deposit because they have similar host rocks, such as those in the Awband and Green Schist Formations.

7A.12.1 Khaish Iron Prospect

The Khaish iron prospect is located at longitude 34°43'55" N. and latitude 68°12'30" E., on the upper reaches of the Khaish River (left tributary of Turkman River), on the south slope of a small ridge 4.5 km to the southwest of Khaish village (fig. 7A–28). The occurrence is 8 km to the south from the road (Khaish-Chorde-Gorband). At the Khaish prospect, five prospects smaller than Khaish have been delineated to date that are 300- to 1,300-m-long and 10- to 20-m-thick and can be traced downdip for 200 m. Speculative resource estimates at Khaish suggest that the deposit may contain up to 117 Mt, but at the low grades of 48.6 wt. % iron, 0.1 wt. % titanium, and 0.019 wt. % cobalt.

The Khaish prospect contains five orebodies comprising blocky fragments of hematite-magnetite ore hosted in the Awband Formation. The orebodies are hosted in different lithologies and along different contacts. Orebody 1 lies along a contact with dolomitic limestone, orebodies 2 and 5 are hosted in sericite and quartz-sericite schist, orebody 3 is hosted along a contact with carbonate-chlorite schist; and orebody 4 is hosted along a contact between quartz-sericite schist and carbonate-chlorite-sericite. The contacts between the orebodies and the schist are sharp and planar, but contacts with dolomitic limestone are more diffuse and gradational (Kusov and others, 1965b).

Orebodies are lenticular, and at places, they conformably overlay host rocks (orebodies 2, 4, 5) or cut through the host rocks (orebodies 3, 4). The length of the orebodies varies from 300 to 1,300 m along the strike and as much as 200 m downdip (erosion), and the width varies from 10 to 200 m. Orebody 1 extends 300 m along the strike and 200 m downdip (stripped by erosion)is 200 m thick from surface to the middle part, and it is pinching out to the flanks. The azimuth of the dip of the orebodies is 95° (orebody 3) and 160° to 175° (orebodies 1, 2, 4, and 5), and the angle of dip is 60° to 70°. The orebodies form a ridge as much as 15 to 20 m high. Fragmental ores are located to the south from natural ores (Kusov and others, 1965b).

The orebodies consist of massive and massive-banded oxidized hematite-magnetite ores with medium- and fine-grained texture and include pores. The rocks contain relicts of pyrite, which indicate the presence of sulfides in nonoxidized ore at the depth. The mineral content of the ore is listed in table 7A–6.

Ores in the Khaish iron prospect are highly oxidized, and contain anomalous concentrations of cobalt and iron. The total length of the orebodies is 2,925 m, the average thickness is 50 m thick, the depth along the dip is 200 m, the volumetric weight is 4.0, and the amount of inferred (prospective ore) resource is 117 Mt (Kusov and others, 1965b).

Table 7A–6. Mineral content of the ore from the Khaish iron prospect.

[Data are from Kusov and others (1965b). Al_2O_3, aluminum oxide; BaO, barium oxide; CaO, calcium oxide; Co, cobalt; Fe, iron; FeO and Fe_2O_3, iron oxide; MgO, magnesium oxide; MnO, manganese oxide; P_2O_5, phosphorus pentoxide; S, sulfur; SiO_2, silicon oxide; TiO_2, titanium oxide; wt. %, weight percent]

Mineral	Content, in wt. %
Fe	48.12–62.97
Fe_2O_3	56.23–77.79
FeO	1.42–12.34
SiO_2	4.00–7.28
Al_2O_3	0.20–1.24
TiO_2	0.023–0.11
CaO	0.22–0.57
MgO	0.045–0.43
MnO	0.057–1.38
BaO	0.0–1.53
Co	0.07–0.019
P_2O_5	0.0–0.28
S	0.03–2.92
Lost in tempering	1.29–7.45

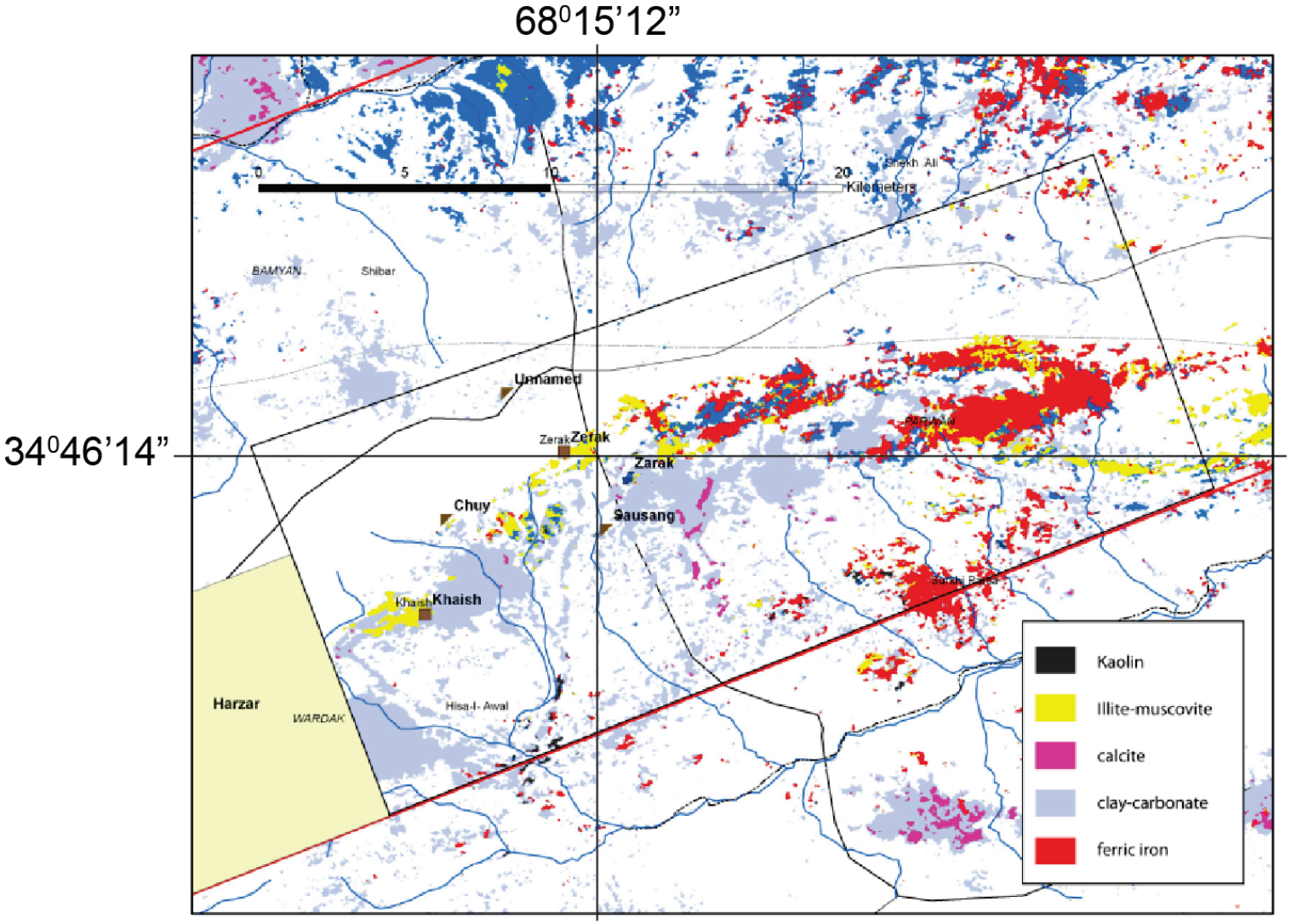

Figure 7A–26. Advanced Spaceborne Thermal Emission and Reflection (ASTER) radiometer image of the Northeastern Haji-Gak subarea showing known iron occurrences and prospects in relation to ASTER mineral anomalous zones. Data from Peters and others (2007).

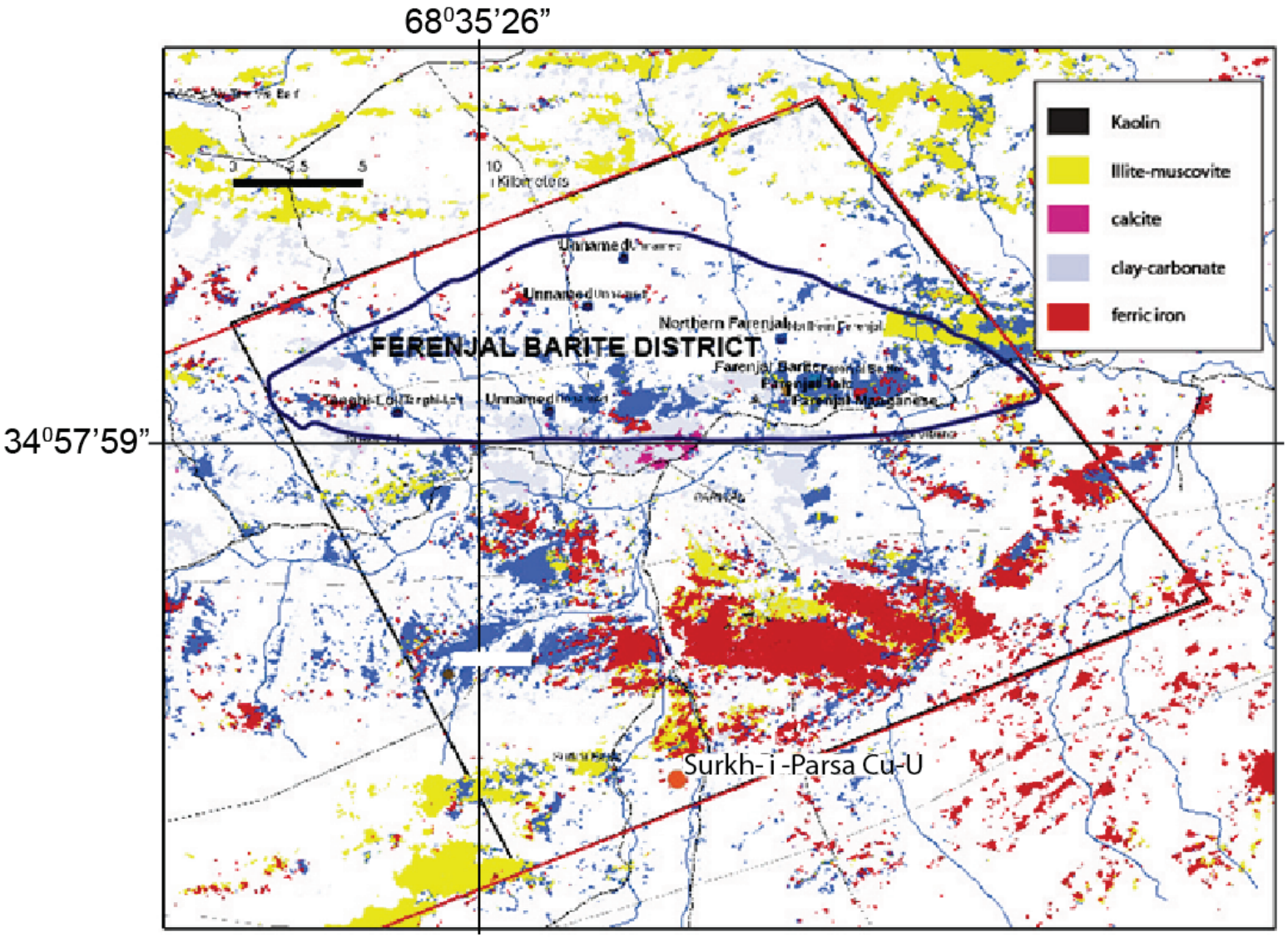

Figure 7A–27. Advanced Spaceborne Thermal Emission and Reflection (ASTER) radiometer image showing the Farenjal barite subarea, which contains the Farenjal barite district in the north and the Surkh-i-Parso copper and uranium occurrence in the south. Data from Peters and others (2007)

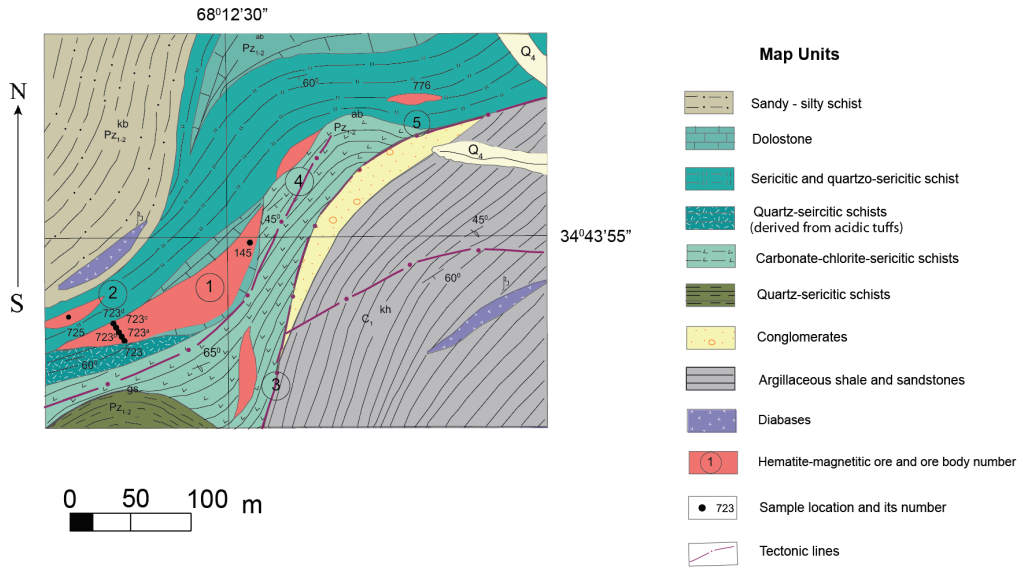

Figure 7A–28. Map of the Khaish deposit, modified from a 1:25,000 map from Kusov and others (1965b).

7A.12.2 Kharzar Iron Prospect

The Kharzar iron prospect is located at longitude 34°41′ 46" N. and latitude 68°09'12" E., along the upper reaches of the Kharzar River, 1.2 km to the south from the Surhan path (fig. 7A–29). Kharzar iron occurrence lies in Proterozoic greenschist rocks and contains 70-m-wide and about 300-m-long hematite lenses grading up to 62.97 wt. % iron. The ore is hosted in the Green Schist Formation and comprises exposed natural ores and fragmental hematite-magnetite ores. The orebodies form lenticular shapes, which are 315 m long along the strike, 70 m wide, and pinch out along the flanks. The fragmental orebodies are located near the natural ores. The orebodies are hosted in quartz-sericite-chlorite schist of the Green Schist Formation with different contacts; the ore and footwall contact with the host rocks is conformable, but the hanging wall contact is cross cutting. The azimuth of the orebody is 170°, and the dip angle is 70° (Kusov and others, 1965b).

The orebody comprises massive or massive-banded hematite-magnetite and martitized ores with fine-grained texture. Secondary pores appear within massive texture. Pyrite relicts are preserved. The mineral content of the ore is listed in table 7A–7.

Table 7A–7. Mineral content of the ore from the Kharzar iron prospect.

[Data are from Kusov and others (1965b). Al_2O_3, aluminum oxide; BaO, barium oxide; CaO, calcium oxide; Co, cobalt; Fe, iron; FeO and Fe_2O_3, iron oxide; MgO, magnesium oxide; MnO, manganese oxide; P_2O_5, phosphorus pentoxide; S, sulfur; SiO_2, silicon oxide; TiO_2, titanium oxide; wt. %, weight percent]

Mineral	Content, in wt. %
Fe	62.55–62.97
Fe_2O_3	70.73–72.61
FeO	15.25–17.71
SiO_2	7.42–10.68
Al_2O_3	as much as 0.37
TiO_2	0.032–0.043
S	0.011–0.11
MgO	0.045–0.23
CaO	0.17–0.25
MnO	0.042–0.076
BaO	0.02–0.032
Co	0.08–0.015
P_2O_5	0.074–0.4
Lost in tempering	0.85–1.71

7A.12.3 Chuy Iron Prospect

The iron-bearing Chuy prospect is located at longitude 34°45'37" N. and latitude 68°13'00" E., in the upper Chuy River. The Chuy iron prospect is 400 m long and 2.5 to 10 m wide and comprises a hematite-magnetite stratabound body within quartz-chlorite schist. The distance from the deposit to the road is 10 km. The ore deposit consists of one orebody, which comprises exposed and oxidized natural hematite-magnetite ore. The orebody is conformable with quartz-chlorite schist of the Awband Formation, the azimuth of dip is 190°, and the angle is 70°. The host rock for the orebody is the quartz-sericite schist. The content and structure of the ore is similar to Kharzar ore deposits. The ore content varies from 48.12 to 65.74 wt. % iron (Kusov and others, 1965b).

7A.12.4 Zerak Iron Prospect

The Zerak iron prospect is located at longitude 34°46'36" N. and latitude 68°15'12" E., in the upper reaches of the Burchistah River (left tributary of Turkman River) on the southern part of Koh-e-Baba Ridge in Baghlan Province. The Zerak iron prospect lies within a fault zone, and three 90- to 450-m-long and 12- to 75-m-wide hematite magnetite zones have been discovered to date. Speculative resources are 20 Mt of iron ore grading as much as 62.5 wt. % iron. The deposit contains three orebodies, the western, central, and eastern orebodies, which are hosted in the Awband Formation. The orebodies are platy, 90 to 450 m long along the strike, and 12 to 75 m thick. The largest orebody is located in the eastern part of the deposit; it is 450 m long along the strike, 75 m wide, and 450 m stripped by erosion along the dip. The three orebodies extend to the northeast, dipping southeast (140° to 160°); the dip angle is 75° to 80°.(Kusov and others, 1965b).

The central and western orebodies were conformably deposited in dolomitic limestone, and the contact is wavy. The eastern orebody footwall comes into contact with schist (derived from tuff), and the hanging wall comes into contact with quartz dolomite. The contact of the eastern orebody with schist is sharp and cross-cutting; with quartz dolomites, it is gradual. The fragmental ore occupies an area of 50 km^2 and is located near the natural ore. The natural ore and fragmental ore comprise hematite-magnetite oxidized ore with massive and medium-grained texture with pores. The small pores are dispersed, and constitute up to 15 percent of the volume. The pore shape is irregular, the surface is covered by ore ochre, and the pyrite relicts are preserved. The mineralogy of the Zerak ore deposit is similar to that of the Kharzar deposit. The prospective ore reserve of Zerak deposit is 20 Mt (Kusov and others, 1965b).

7A.12.5 Khakriz Iron Prospect

The Khakriz iron prospect is located 5 km to the east of Zerak, 2.5 km to the south of the Shagdar path, and is connected by the Turkman valley (6 km long), the Kabul-Gorband road (24 km long), and by trails. The ore outcrops as hematite (probably martite). The size, depositional conditions, and other aspects of the ore deposit are unknown (Manucharyants and others, 1963).

7A.12.6 Sausang Iron Prospect

The Sausang iron prospect is located at latitude 34°45'08" N. and latitude 68°15'45" E., 2.2 km to the south of the Zerak iron prospect on the right slope of Burchistah River, to the west of the Sausang path (Abdullah and others, 1977). The prospect contains one small lenticular orebody, which outcrops along the top of the mountain and lies conformably in or on quartz-chlorite-sericite schist (derived from tuff and volcanic rocks). The contact of the ore with the schist is sharp and straight. The schist has been altered by seritization and silicification. The orebody outcrop is 350 m long and 15 m thick, the dip azimuth is 160°, and the angle is 60°. The orebody comprises hematite-magnetite ores similar to ores of the Zerak deposit.

7A.12.7 Darre-i-Neel Iron Prospect

The Darre-i-Neel prospect is located at longitude 34°54' N. and latitude 68°34' E., in the upper reach of the Darre-i-Neelee stream, 9 km northeast of the Khakriz deposit. The ore comprises individual exposed ores and blocky martite float, which formed in skarns. The size, content, and depositional conditions of this ore deposit are unknown (Manucharyants and others, 1963; Kusov and others, 1965a,b; Chmyriov and others, 1973).

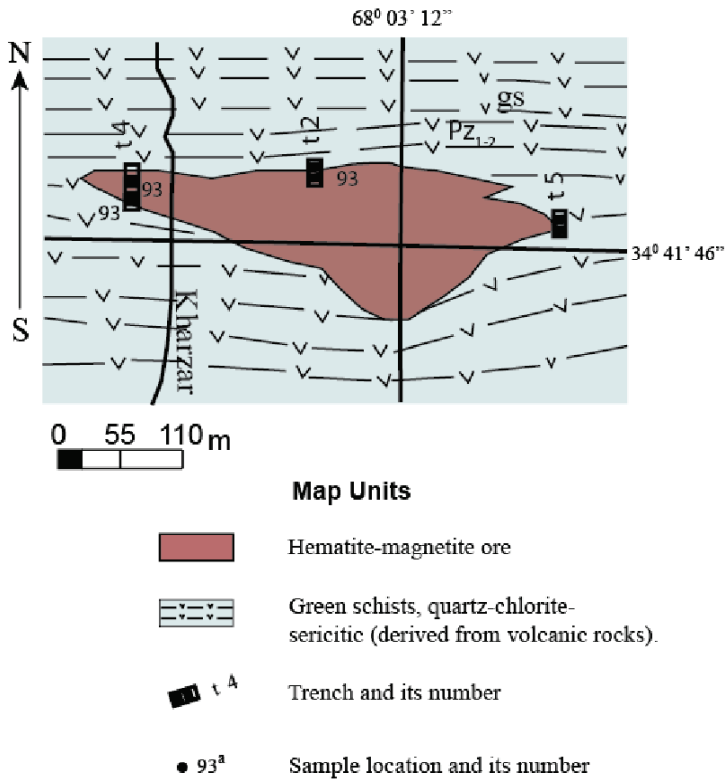

Figure 7A–29. Schematic plan showing the Kharzar deposit, modified from a 1:5,000 schematic from Kusov and others (1965b).

7A.12.8 Surkh-o-Parso Iron Prospect

Surkh-o-Parso is located at longitude 34°51' N. and latitude 68°39' E. near the mouth of the Turkman River, 30 km to the east from Darre-i-Neel. The region is connected with Gorband City by a winding path (11 km long). Blocky fragments of hematite-magnetite ore constitute the ore deposit; the size and depositional conditions are unknown. The Surkh-o-Parso prospect and ore manifestations are related to the same structure and suite of metamorphic rocks. Besides iron ores, lead-zinc-barite ores also are present in this area (Manucharyants and others, 1963). Disseminated chalcopyrite has been found over an area of 9 km^2 in marmorized limestone and quartzite of Carboniferous to Early Permian age. Uranium minerals also have been found at the occurrence (Khananov and others, 1967).

7A.12.9 Farenjal Barite Subarea

The Farenjal barite subarea contains barite deposits and occurrences in Paleozoic rocks and the Surkh-o-Parso iron-copper-uranium prospect (fig. 7A–30) (Abdullah and others, 1977). The Farenjal barite and lead-zinc ore district lies along the Gorband River basin, in an area underlain by Paleozoic carbonate-shale and volcanic rocks. The area is known for barite, lead, and zinc mineralization. The subordinate mineralization is represented by manganese, iron, copper, talc, and asbestos. The deposits and occurrences of the barite and lead-zinc ore formation are usually found in shear zones within Lower Carboniferous terrigenous-carbonate rocks feathering the Har-i-Rod Fault. The tops of the carbonate

barite veins are almost devoid of lead and zinc sulfides. From a depth of 100 m downdip, the calcite-barite ore grades into calcite-sulfide ore that is poor in barite and rich in lead and zinc. Stream sediment sampling revealed rich haloes of gold and cinnabar with scheelite, wolframite, and cassiterite. The source of these minerals is unknown.

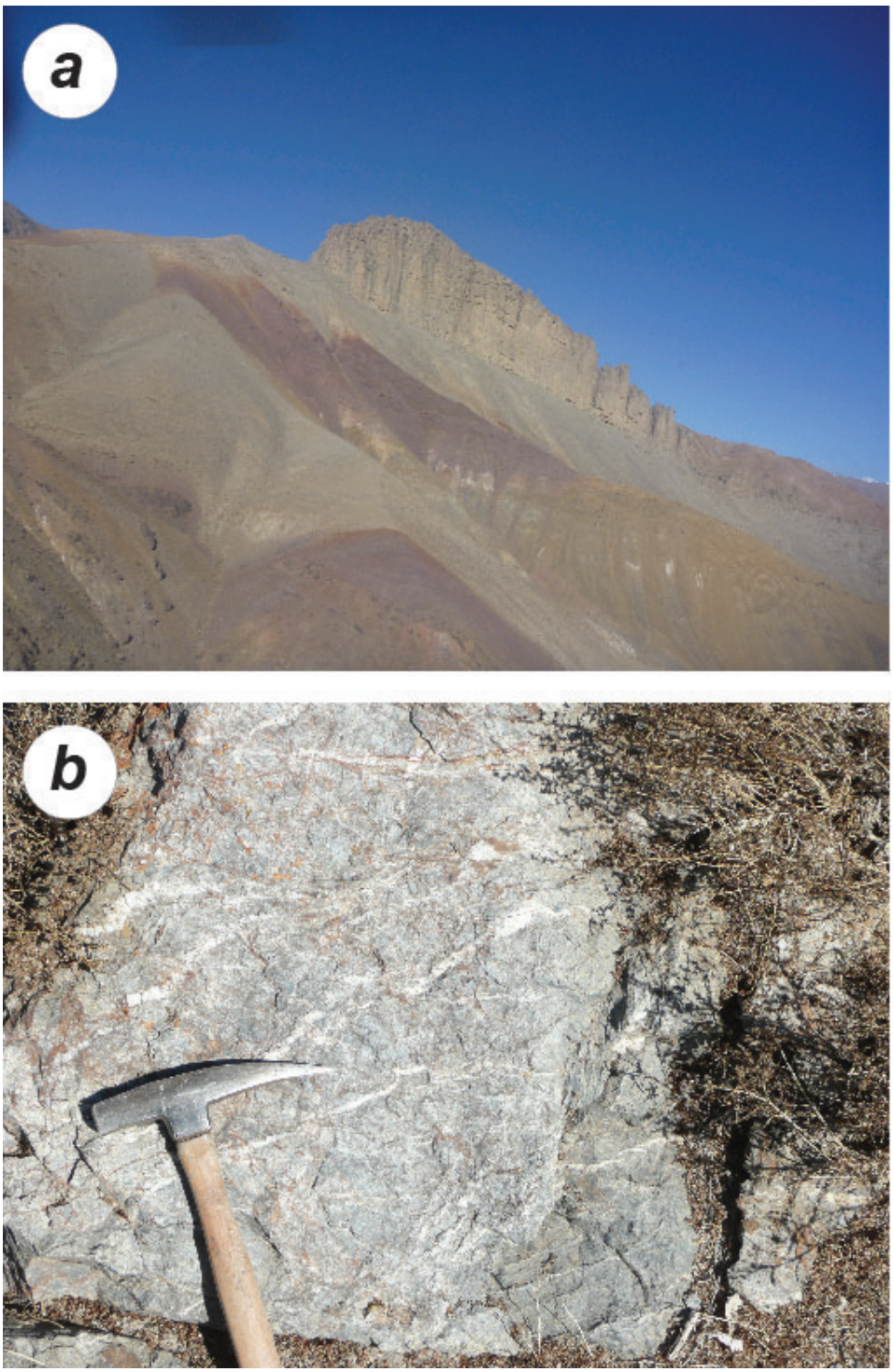

Figure 7A–30. Photographs of the Surkh-o-Parso copper-uranium prospect in the Haji-Gak iron area of interest. (*a*) North view of the Phanerozoic sequence at Surkh-o-Parso showing the northward dip of the sedimentary strata. (*b*) Photograph of whispy discontinuous quartz-pyrite veins in a 2-meter-wide zone. Photographs are by Robert Bohannon, U.S. Geological Survey.

7A.13 Summary of Potential

The Haji-Gak iron AOI contains the Haji-Gak iron deposit, a world class-size deposit, and several other iron prospects. Three subareas have been delineated within the main AOI that have additional potential for economic deposits. The Haji-Gak iron deposit is more than 32 km long and contains 16 separate zones, some of which are up 15 km long, 380 m wide, and extend 550 m downdip. Seven of these zones have been studied in detail. Previous Russian resource estimates for the entire deposit are 1,700 Mt. The Kharzar, Khaish, Chuy, Khakriz, and Zerak sedimentary-rock-hosted iron deposits are adjacent to and to the east of the main Haji-Gak iron deposit in the Northeastern Haji-Gak subarea and have also been explored. The Haji-Gak iron AOI also contains barite deposits and mineralization near the Haji-Gak prospect subarea and in the Farenjal subarea in the northeast of the AOI. The subordinate mineralization is represented by manganese, iron, copper, talc, and asbestos. Additionally, the Haji-Gak prospect subarea contains the Haji-Gak limestone deposit, which contains 3.5 Mt of speculative resources in an area of 45 km^2 to a depth of 60 m. The Haji-Gak sandstone deposit, also in the Haji-Gak prospect subarea, contains 650,000 t of speculative resources with a silicon oxide content of 93.66 to 97.31 vol. %.

7A.14 Selected References

Abdullah, S.H., Chmyriov, V.M., Stazhilo-Alekseyev, K.F., Dronov, V.I., Gannan, P.J., Rossovskiy, L.N., Kafarskiy, A.Kh., and Malyarov, E.P., 1977, Mineral resources of Afghanistan (2d ed.): Kabul, Afghanistan, Afghanistan Geological and Mineral Survey, 419 p.

Afghanistan Geological and Mineral Survey, 1967, Geological structure of the Haji-Gak iron deposit and its commercial value:: Kabul, Afghanistan, Afghanistan Geological and Mineral Survey13 p.

Bekker, Andreyndrey, Slack, J.F., Planavsky, Noah, Krapez, Bryanryan, Hofman, Axel, Konhauser, K.O., and Rouxel, O.J., 2010, Iron formation—The sedimentary products of a complex interplay among mantle, tectonic, oceanic, and biospheric processes: Economic Geology, v. 105, p. 467–508

Bouladon, Jean, and de Lapparent, A.F., 1975, Le minerai de fer d'Hajigak (Afghanistan); position stratigraphique, cadre géologiqué et type du gisement [The iron minerals of the Haji-Gak Pass, Afghanistan; stratigraphic position, geological evolution and type of deposit]: Mineralium Deposita, v. 10, no. 1, p. 13–25.

Brice, D., de Lapparent, A.F., and Mistiaen, Bruno, 1974, Le Devonien superieur a l'est d'Hajigak (Afghanistan) [The upper Devonian east of Hajigak, Afghanistan]: Annales de la Société Geologique du Nord, v. 94, no. 2, p. 67–70.

British Geologic Survey, [na], Minerals in Afghanistan [The Hajigak iron deposit], Afghan Geological Survey, http://www.bgs.ac.uk/AfghanMinerals/docs/Hajigak_A4.pdf, p. 1-6.

Brueckl, K., 1935b, Über die geologie von Badakhshan und Kataghan (Afghanistan)[The geology of Badakhshan and Kataghan (Afghanistan)]: Neues Jahrbuch für Mineralogie, Geologie und Paläontologie, v. 74, pt. B, no. 3, p. 360–401.

Brueckl, K., 1936, Die minerallagerstaetten von Ostafghanistan; versuch einer gliederung nach genetischen gesichtspunkten [The mineral regions of east Afghanistan; their origins and characteristics]: Neues Jahrbuch für Mineralogie, Geologie und Paläontologie, Abhandlungen, pt. A, Mineralogie, Petrographie, v. 1, p. 1–97.

Bybochkin, A.M., and Kats, Ya.G., 1970, Rezul'taty geologicheskikh issledovaniy, vypolnennykh sovetskimi geologami v stranakh Blizhnego i Srednego Vostoka, Pakistane i Indii [Geologic studies done by Soviet geologists in Near and Middle East countries, Pakistan and India]: Izvestiya Vysshikh Uchebnykh Zavedeniy, Geologiya i Razvedka, v. 10, p. 3–11.

Bybochkin, A.M., and Kurotchenko, V. , 1960, Report on preliminary geological-economic evaluation of minerals of Afghanistan and recommendation on orientation of geological-reconnaissance works for the second five-year plan: Kabul, Afghanistan, Afghanistan Geological and Mineral Survey, [unpaginated].

Cannon, W.F., 1986a, Descriptive model of Algoma Fe, *in* Cox, D.P., and Singer, D.A., eds., Mineral deposit models: U.S. Geological Survey Bulletin 1693, p. 198.
Cannon, W.F., 1986b, Descriptive model of Superior Fe, *in* Cox, D.P., and Singer, D.A., eds., Mineral deposit models: U.S. Geological Survey Bulletin 1693, p. 228.
Chmyriov, V.M., Stazhilo-Alekseyev, K.F., Mirzad, S.H., Dronov, V.I., Kazikhani, A.R., Salah, A.S., and Teleshev, G.I., 1973, Mineral resources of Afghanistan, *in* Geology and mineral resources of Afghanistan (1st ed.): Kabul, Afghanistan, Afghanistan Geological and Mineral Survey, p. 44–86.
Cox, D.P., 1986, Descriptive model of Olympic Dam Cu-Au-U, *in* Cox, D.P., and Singer, D.A., eds., Mineral deposit models: U.S, Geological Survey Bulletin 1693, p. 200.
Demag (Creusot-Loire Industrie S.A.), 1974, Feasibility study for an integrated iron and steel plant in Afghanistan: Duisberg, Germany, Demag, April, [unpaginated].
Gross, G.A., 1973, The depositional environment and principal types of Precambrian iron-formation, *in* Genesis of Precambrian iron and manganese deposits, Proceedings of the Kiev Symposium, 1970: United Nations Educational, Scientific and Cultural Organization Earth Sciences, v. 9, p. 15–21.
Haynes, D.W., 2000, Iron oxide copper gold deposits—Their position in the ore deposit spectrum and modes of origin, *in* Porter, T.M., ed., Hydrothermal iron oxide copper-gold and related deposits—A global perspective: Adelaide, Australian Mineral Foundation, p. 71–90.
Hitzman, M.W, 2000, Iron oxide-Cu-Au deposits—Where, when, and why, *in* Porter, T.M., ed., Hydrothermal iron oxide copper-gold and related deposits—A global perspective: Adelaide, Australian Mineral Foundation, p. 9–25.
Karapetov, S.S., Stazhilo-Alekseyev, K.F., and Kotchetkov, A.Ya., 1970, The geology and minerals of the eastern part of central Afghanistan: Kabul, Afghanistan, Afghanistan Geological and Mineral Survey, [unpaginated].
Khananov, R.M., Plotnikov, G.I., Bayazitov, R.A., Sayapin, V.I., and Trifonov, A.I., 1967, Report on revised estimation investigations of mineral deposits and occurrences of copper, lead, zinc and gold in 1965——V. I–II:: Kabul, Afghanistan, Afghanistan Geological and Mineral Survey, [unpaginated].
Kirst, E., 1925, Mining program for the Paghman iron ore deposit: Kabul, Afghanistan, Afghanistan Geological and Mineral Survey, [unpaginated].
Kusov, I.K., 1963, Geological mapping, prospecting, and exploration on the iron deposit of Hajigak: Kabul, Afghanistan, Afghanistan Geological and Mineral Survey USSR v/o Technoexport contract no. 640, 88 p
Kusov, I.K., Smirnov, M.S., and Reshetnyak, V.V., 1965a, Report on prospecting and survey at iron occurrences in central Afghanistan and the Hajigak iron deposit's estimated reserves: Kabul, Afghanistan, Afghanistan Geological and Mineral Survey, [unpaginated].
Kusov, I.K., Smirnov, M.S., and Reshetnyak, V.V., 1965b, Report on the results of geological prospecting, survey and exploration of iron deposits and occurrences in central Afghanistan with the data on iron ore reserves estimation of the Haji-Gak deposit carried out in 1963–1964: Kabul, Afghanistan, Afghanistan Geological and Mineral Survey USSR v/o Technoexport contract no. 640, 3 v., [variously paginated].
Lapparent, A.F. de, Bouladon, J., and de Lavigne Sainte-Suzanne, J., 1964, Nouvelles donnees sur le minerai de fer d'Hajigak en Afghanistan: Comptes Rendus Hebdomadaires des Séances de l'Académie des Sciences, v. 259, no. 5, p. 1153–1154.
Lapparent, A.F. de, 1971, Essai sur le Paleozoique de la region d'Hajigak, Afghanistan, et son encadrement [The Paleozoic of the Hajigak region, Afghanistan, and its surroundings]: Annales de la Société Géologique du Nord, v. 91, no. 2, p. 145–154.
Manucharyants, O., Mirzad, S.H., and Kusov I.K., 1963, Project of geological survey, prospecting, and exploration works on iron ores of the Hajigak deposit: Kabul, Afghanistan, Afghanistan Geological and Mineral Survey, [unpaginated].
Ministry of Mines and Industries, 1965, General information on Hajigak ore deposits: Kabul, Afghanistan, Afghanistan Geological and Mineral Survey, [unpaginated].

Mirzad, S.H., 1961, Iron ore deposit of the Hajigak pass: Jundun, no. 26, appendix, [unpaginated].
Momji, G.S., and Chaikin, S.I., 1960, Iron ores of Afghanistan: Kabul, Afghanistan, Afghanistan Geological and Mineral Survey, [unpaginated].
Nishiwaki, Chikao, 1970, Iron ore deposits of the Middle East, Asia and the Far East, *in* Survey of world iron ore resources—Occurrence, appraisal and use: United Nations Committee of Experts on Iron Ore Resources, p. 102–206.
Peter, J.M., 2010, Hydrothermal influences on iron formation genesis, *in* Geology, mineralogy, and genesis of Precambrian iron formations, Duluth, Minn., October 10–16, 2010: Precambrian Research Center, University of Minnesota Duluth, Presentation, 36 p.
Peters, S.G., Ludington, S.D., Orris, G.J., Sutphin, D.M., Bliss, J.D., and Rytuba, J.J., eds., and the U.S. Geological Survey-Afghanistan Ministry of Mines Joint Mineral Resource Assessment Team, 2007, Preliminary non-fuel mineral resource assessment of Afghanistan: U.S. Geological Survey Open-File Report 2007–1214, 810 p., 1 CD–ROM. (Also available at *http://pubs.usgs.gov/of/2007/1214/*.)
Popol, S.A., and Tromp, S.W., 1954, The stratigraphy and main structural features of Afghanistan: Koninklijke Nederlandische Academie von Wetenschappen Proceedings, Series B, v. 57, no. 3, p. 370–394.
Renaud, K.M., Tucker, R.D., Peters, S.G., Stettner, W.R., Masonic, L.M., and Moran, T.W., comps., 2011a, Geologic map of the Haji-Gak iron deposit, Bamyan Province, Afghanistan, modified from the 1965 original map compilation of M.S. Smirnov and I.K. Kusov: U.S. Geological Survey Open-File Report 2011–1185–A, one sheet, scale 1:10,000, available at *http://pubs.usgs.gov/of/2011/1185/A/*.
Renaud, K.M., Tucker, R.D., Peters, S.G., Stettner, W.R., Masonic, L.M., and Moran, T.W., comps., 2011b, Geologic map of the western Haji-Gak iron deposit, Bamyan Province, Afghanistan, modified from the 1965 original map compilation of V.V. Reshetniak and I.K. Kusov: U.S. Geological Survey Open-File Report 2011–1185–B, one sheet, scale 1:4,000, available at *http://pubs.usgs.gov/of/2011/1185/B/*.